

FLORISTICS OF HARDING LAKE, ALASKA

Thesis for the Degree of M. S.
MICHIGAN STATE UNIVERSITY
FREDERICK CARROLL PAYNE
1977

FLORISTICS OF HARDING LAKE, ALASKA

By

Frederick Carroll Payne

A THESIS

Submitted to
Michigan State University
in partial fulfillment of the requirements
for the degree of

MASTER OF SCIENCE

Department of Fisheries and Wildlife

1977

ABSTRACT

FLORISTICS OF HARDING LAKE, ALASKA

By

Frederick Carroll Payne

Fifteen vascular hydrophyte and one macrophytic algal taxa were found to inhabit Harding Lake, a deep, highly oligotrophic lake of the unglaciated Alaskan subarctic. Two emergent and three floating-leaved species were present at relatively low densities while eleven submergent taxa formed the dominant communities. Macrophytic growth was limited to the 0-4.2 meter depth zone with large areas of this zone totally uncolonized. The distribution of submersed hydrophyte growth forms in the lake is considered to have been determined by patterns of wave action, siltation and substratum texture and by light and temperature regimes.

FLORISTICS OF HARDING LAKE, ALASKA

By

Frederick Carroll Payne

A THESIS

Submitted to
Michigan State University
in partial fulfillment of the requirements
for the degree of

MASTER OF SCIENCE

Department of Fisheries and Wildlife

1977

ACKNOWLEDGMENTS

I sincerely thank Dr. C. D. McNabb for his guidance and assistance during his time as my major advisor.

My graduate committee, Professors R. A. Cole and K. W. Cummins, was helpful in discussing my project and reviewing this thesis.

I greatly appreciate the efforts of my wife, Therese, who travelled to Alaska with me and supported and encouraged me through the completion of this project.

Discussions with my fellow graduate students aided the development of my ideas. I am especially grateful to Robert Glandon for his critical reviews at various stages of this project.

The Institute of Water Research at the University of Alaska provided logistic support for my project at Harding Lake. Special thanks go to Tim Tilsworth and Jacqueline LaPerriere for their assistance during my work.

My graduate program was supported by an E.P.E.-O.W.P. Training Grant (T-900331). My travel to Alaska was supported in part by the Foundation for Environmental Education.

TABLE OF CONTENTS

	Page
LIST OF TABLES	iv
LIST OF FIGURES	v
INTRODUCTION	1
DESCRIPTION OF THE STUDY AREA	2
METHODS	7
RESULTS	9
Characeae	9
<u>Isoetes muricata</u> var. <u>Braunii</u>	14
<u>Sparganium angustifolium</u>	18
<u>Potamogeton filiformis</u>	21
<u>P. Friesii</u>	22
<u>P. gramineus</u>	25
<u>P. natans</u>	25
<u>P. perfoliatus</u> subsp. <u>Richardsonii</u>	32
<u>P. praelongus</u>	35
<u>Glyceria borealis</u>	40
<u>Eleocharis acicularis</u>	40
<u>E. palustris</u>	43
<u>Polygonum amphibium</u>	43
<u>Ranunculus confervoides</u>	43
<u>Subularia aquatica</u>	44
<u>Myriophyllum</u> sp.	44
DISCUSSION	48
LITERATURE CITED	53
APPENDICES	56
Appendix I	57
Appendix II	95

LIST OF TABLES

Table		Page
A-1	The sun's declination throughout the year (degrees) .	66

LIST OF FIGURES

Figure	Page
1. The location of Harding Lake and Yukon and Tanana Rivers	3
2. Plant distributions in Harding Lake, 1974. The positions of transects used to characterize the areas of major hydrophyte colonization are shown . .	10
3. Growth habits of Harding Lake specimens of <u>Chara</u> sp. Rhizoids were present, but are not shown here . . .	12
4. Growth habits of <u>Isoetes muricata</u> var. <u>Braunii</u> in Harding Lake, showing rosette of fronds originating from hardened, reduced stem. Long dichotomously branching roots penetrate the substratum	12
5. Physiognomy of hydrophyte species populations in Harding Lake: (a) <u>Eleocharis acicularis</u> , transect 1; (b) <u>Isoetes muricata</u> var. <u>Braunii</u> , transect 1; and (c) <u>Potamogeton filiformis</u> , transect 5	16
6. Growth habits of <u>Sparganium angustifolium</u> in Harding Lake, showing floating leaves and flowers, originating from a long, slender stem. Roots are many, unbranching; plants without rhizomal system . .	19
7. Growth habits of <u>Potamogeton filiformis</u> , depicting long, filiform leaves and seeds borne in one or two whorls, on elongated peduncles, with taproot extending downward to tuber. Secondary shoots are seen along rhizomal system	19
8. Growth habits of <u>Potamogeton Friesii</u> in Harding Lake showing root and shoot extension from winter bud above substratum	23
9. Physiognomy of hydrophyte species populations in Harding Lake: (a) <u>Potamogeton gramineus</u> , transect 5; (b) <u>Potamogeton perfoliatus</u> subsp. <u>Richardsonii</u> , transect 5; (c) <u>Potamogeton praelongus</u> , transect 5 . .	26

Figure	Page
10. Growth habits of <u>Potamogeton gramineus</u> , deep-water form, in Harding Lake, showing spike of seeds on elongate peduncle, numerous submersed leaves and rhizomal system with taproot extending downward to tuber	28
11. Growth habits of shallow-water form of <u>Potamogeton gramineus</u> in Harding Lake, showing floating leaves, rhizomal system and taproot extending downward to tuber	30
12. Growth habits of <u>Potamogeton perfoliatus</u> subsp. <u>Richardsonii</u> , deep-water form, in Harding Lake, depicting branching shoots with flower spikes and extensive rhizome and secondary shoot system	33
13. Growth habits of <u>Potamogeton perfoliatus</u> subsp. <u>Richardsonii</u> , shallow-water form, in Harding Lake, showing compacted stem, spike of seeds and extensive rhizome and secondary shoot system	36
14. Growth habits of <u>Potamogeton praelongus</u> in Harding Lake, showing large leaves on branching stem, flower spikes below the water surface and strong rhizomal system with secondary shoots	38
15. Growth habits of <u>Glyceria borealis</u> in Harding Lake, depicting rhizomal system development with mature spikes rising above the water surface	38
16. Growth habits of <u>Eleocharis acicularis</u> in Harding Lake, depicting fertile form growing in isolated tufts and the much smaller sterile form, growing along an extensive rhizomal system	41
17. Growth habits of <u>Ranunculus confervoides</u> in Harding Lake, showing small tuft of plant resting in substratum depression. Small roots are present, but do not penetrate the sediment surface. Seeds are borne in achenes	41
18. Growth habits of <u>Subularia aquatica</u> in Harding Lake, showing whorl of leaves growing from reduced stem, tuft of unbranching roots and flowers and seed capsules growing on long peduncles	45

Figure	Page
19. Growth habits of <u>Myriophyllum</u> sp. in Harding Lake, showing new roots and shoots growing from previous year's winter buds. Roots can be seen to penetrate the sediment surface	45
A1. Solar spectral irradiance incident to a surface perpendicular to the path of the light at the top of the earth's atmosphere (redrawn from Gates, 1962) .	61
A2. The celestial sphere, relating variables necessary for the calculation of the sun's path through the sky	63
A3. The effect of absorbing area of a receiving surface when the angle of incidence is non-zero	70
A4. Refraction of light at the air-water interface, showing the relationships of incident, reflected and refracted light	73
A5. Path of the sun through the sky on June 22 at Harding Lake and Lake Lansing, Michigan	79
A6. Path of the sun through the sky on the summer solstice day throughout the northern hemisphere	85
A7. The influence of the sun's angular elevation on the solar irradiance at 440-450 and 660-670 nm which reaches the 0- and 4-meter depths in lakes	87
A8. Total solar irradiance in the 440-450 and 660-670 nm wavebands which reaches the 0- and 4-meter depths of lakes at all latitudes of the northern hemisphere on June 22	89

INTRODUCTION

Harding Lake, a deep subarctic lake of the central Alaskan interior, represents a hydrophyte habitat type previously little described. The conditions of light, nutrient dynamics, basin morphometry and thermal regimes are unique to lakes within this unglaciated subarctic region. This study considers the hydrophyte colonization in Harding Lake during June to August, 1974. The distributions of the taxa within the lake, their growth and reproductive habits, and the physiognomy of the taxa and their associations are described. The objective of this study was to determine the relation of aquatic plant growth forms to physical habitat conditions of the lake.

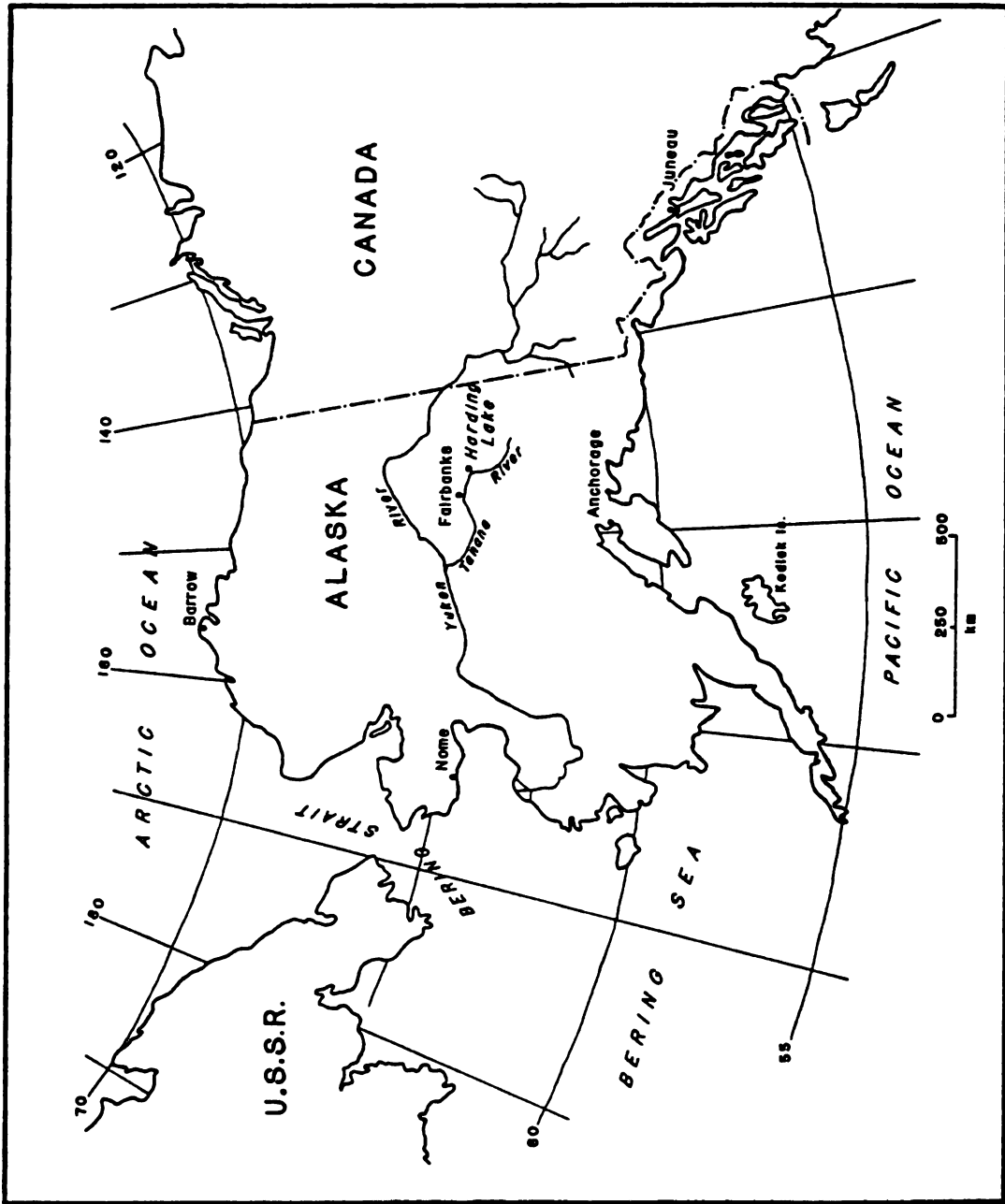
DESCRIPTION OF THE STUDY AREA

The subarctic interior of Alaska is a plateau, bordered on the north by the Brooks Range and to the south by the highest peaks in North America, the Alaska Range. This plateau extends eastward into the upper Yukon River drainage and westward to the Bering Sea. Harding Lake lies in the Tanana River valley at an altitude of 217 meters, lower than the surrounding areas of the plateau which rise to between 600 and 900 meters above mean sea level. The lake is at 64° 25' North Latitude, 146° 50' West Longitude, 2.5° below the Arctic Circle (see Figure 1).

Harding Lake lies in a complex basin which has been described by Blackwell (1964). Shoreline geologic formations include Tanana gravel overlain by silt, colluvial and alluvial silt, and undifferentiated bedrock, along with large areas of beach deposits and reworked alluvium. The genesis of the lake is unclear, but Blackwell (1964) proposes that it formed by the aggradation of the Tanana River and may have been deepened by tectonic activity. The surface level of the lake appears to have undergone drastic fluctuations over the past 75 years which remain unexplained.

The region surrounding Harding Lake has a continental climate, with extreme temperatures and very little precipitation. The highest temperature recorded for this area is 32° Celsius and the lowest is -53° Celsius. The mean July air temperature is near

Figure 1.--The location of Harding Lake and Yukon and Tanana Rivers



15° Celsius while the mean annual air temperature is about -5° Celsius. Precipitation during the terrestrial growing season is 20 centimeters, while the total mean annual precipitation is slightly above 30 centimeters. LaPerriere, et al. (1975) report that the average annual snowfall at Harding Lake is 12.7 centimeters. Only one-third is measurable as runoff from the adjacent portions of the basin.

The lake is roughly circular with a surface area of 1,063 hectares and a perimeter of 12.9 kilometers. The maximum depth is 43 meters and the mean depth is 16.1 meters. Underwater slopes are quite variable throughout the lake, although consistently steep below the 12-meter contour. Minimum slopes are encountered in the northern portion of the lake, where the 4-meter contour is about 800 meters from the shore; maximal slopes are in the southern area, where the 4-meter contour is less than 40 meters from shore.

Wetzel (1975) shows that the daily maximum potential solar energy striking the earth's surface during June and July is higher in arctic and subarctic areas than in the lower, temperate latitudes. LaPerriere, et al. (1975) indicate that the Harding Lake surface receives over 800 calories per square centimeter per day on the summer solstice. This is more than 80 percent of the potential shown in Wetzel (1975). The light regimes influencing the submersed hydrophytes, however, are confounded by many factors. While the daily total incident radiation in the upper atmosphere of the subarctic latitudes is higher than that for the temperate latitudes, the maximum flux at the water's surface is significantly lower. In

fact, atmospheric attenuation, reflection at the air-water interface and the attenuation of incident light by water are increased with increasing latitude. The proof of this is provided in Appendix I.

The water clarity at Harding Lake allows penetration of light to considerable depths. LaPerriere, et al. (1975) show that oceanographic secchi disk (50 centimeter diameter) readings average about 10 meters throughout the ice-free season, while the one percent light transmission level is at the 16-meter depth during the peak of stratification. Sixty-four percent of the lake's volume and fifty percent of the substratum surface area lie in this trophogenic zone.

METHODS

Plant collections were begun at Harding Lake at the beginning of the growing season. Plant collections were made by diving, with great care taken to obtain all portions of the plant buried in the sediment. Specimens were pressed, dried and mounted on herbarium sheets. Identifications were made using taxonomic keys provided by Fasset (1966) and Hulten (1968). Nomenclature follows Hulten (1968). Voucher specimens were deposited at the Aquatic Plant Herbarium, Department of Fisheries and Wildlife, Michigan State University, and the herbarium of the Department of Botany, University of Alaska. The plant distribution map for Harding Lake was compiled after thorough searches of the lake for hydrophyte populations.

Six transects were studied to describe the physiognomy of the major hydrophyte populations of Harding Lake. A nylon rope, 100 meters in length, tagged and labelled every 5 meters, was stretched from the shoreline to an anchored bouy such that the rope was perpendicular to the shoreline and suspended above the submersed plant stands. A diver moved along the line, stopping at each 5-meter mark to observe the total depth as measured by a sounding line. The appearance and texture of the sediment as determined by hand probing, the height of each plant species in the stand as measured by the sounding line, and the percentage cover of each species was

recorded. The cover in the densest stand of each species was designated as 100 percent.

Growth habit drawings were made by the author, using as subjects the mounted herbarium specimens. Each drawing represents one or more of the herbarium specimens, and is intended to represent accurately the structures present in the respective species.

RESULTS

During June through August, 16 taxa of hydrophytes were encountered in Harding Lake. The lakewide distribution pattern is shown in Figure 2. The physiognomy of populations and the growth and reproductive habits for each of the taxa are presented below.

Characeae

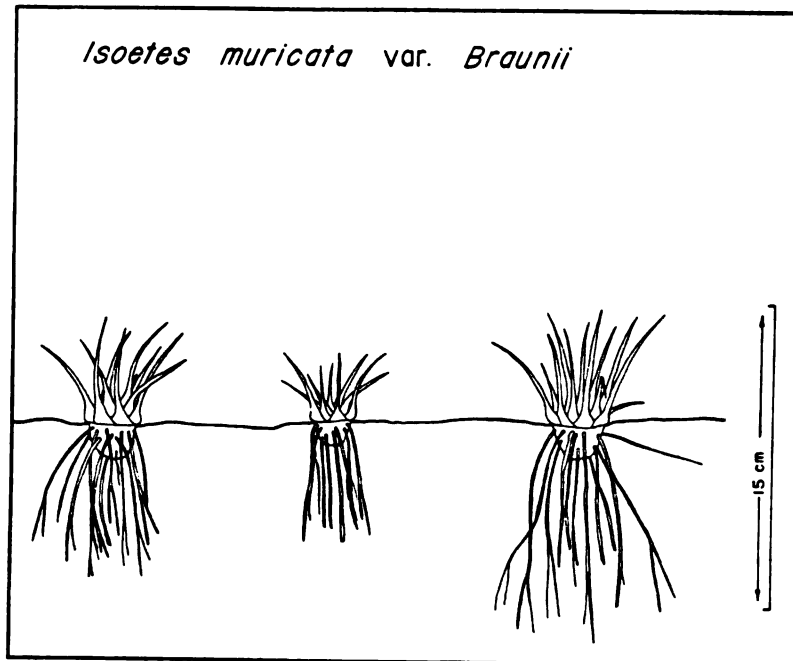
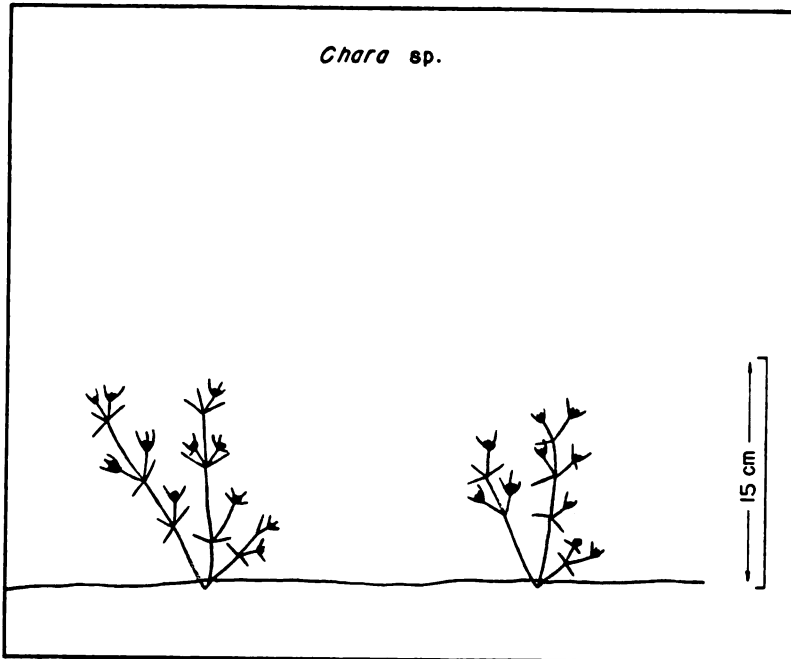
The charophytes of Harding Lake were distributed irregularly throughout the littoral areas of the lake. One major colony of Chara sp. was located by divers in the northwest quadrant of the lake, near similarly monospecific stands of Potamogeton perfoliatus subsp. Richardsonii and P. praelongus. The dotted zone in the northwest quadrant of Figure 2 indicates the area where monospecific stands of all three of the above-mentioned taxa were located. The charophytes were also found scattered through the major hydrophyte colonization zone in the southern littoral area of the lake, and are reported from transects 1, 3 and 5, where they were found infrequently and at very low densities.

In each transect of occurrence, the charophytes were among the two or three taxa of deepest distribution, growing at depths between 240 and 400 centimeters and anchored in sand/silt substrata. In transect 1, the charophytes were found along a very gradual slope at 310 centimeters depth, 100 meters from shore. These were the

Figure 2.--Plant distributions in Harding Lake, 1974. The positions of transects used to characterize the areas of major hydrophyte colonization are shown.

Figure 3.--Growth habits of Harding Lake specimens of Chara sp. Rhizoids were present, but are not shown here.

Figure 4.--Growth habits of Isoetes muricata var. Braunii in Harding Lake, showing rosette of fronds originating from hardened, reduced stem. Long dichotymously branching roots penetrate the substratum.



only plants observed in the sample, with an estimated 50 percent cover and individuals growing to a height of 6 centimeters above the sediment surface. In transect 3, the charophytes were located 95 meters from shore at the 320 centimeter depth on a gradual slope where the plants were again 6 centimeters tall. In this sample, Myriophyllum sp. was also present, both taxa at negligible biomass. In transect 5, the charophytes were located at the 240 centimeter depth, 70 meters from shore on a steep slope, along with Potamogeton perfoliatus subsp. Richardsonii and P. praelongus. Plants in this sample were 10 centimeters tall, with negligible biomass.

The charophytes of Harding Lake all exhibited a branching shootlike system, with whorled leaflike structures at every node and bearing reproductive structures. Figure 3 shows typical specimens collected along the transects. Rhizoid structures provided anchorage and apparently secreted a substance which cemented the sand and silt substratum particles into a hardened matrix, preventing the author from describing further the rhizoid system. All attempts to separate the rhizoids from the matrix resulted in their destruction. Consequently, rhizoids have not been drawn in Figure 3. The plants occurred as small tufts, with filaments first observed on June 15. Nucules were observed in most specimens collected after July 15.

Isoetes muricata Dur. var. Braunii (Dur.) Reed
(Isoetes Braunii Dur. not Unger)

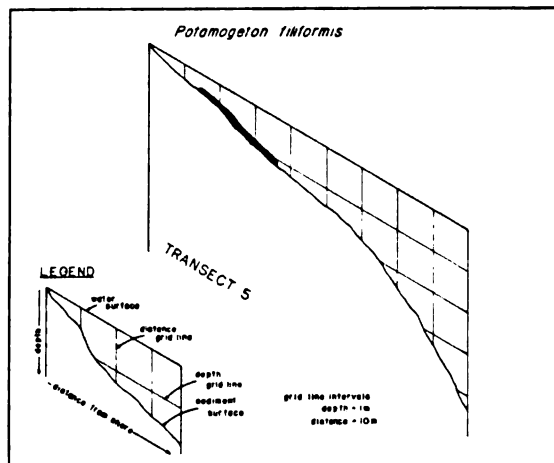
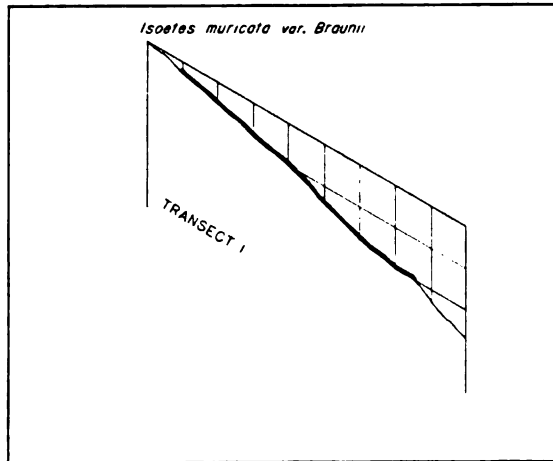
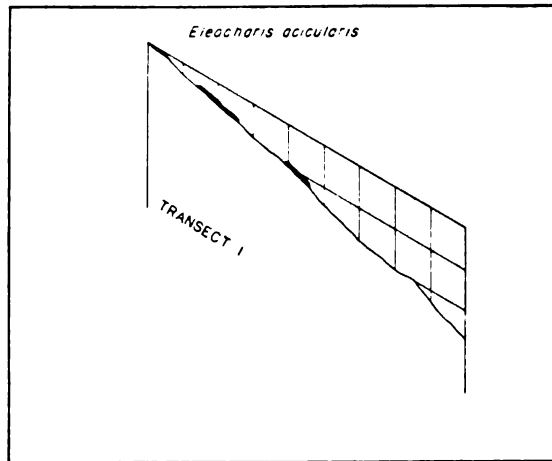
Isoetes muricata var. Braunii, with Potamogeton perfoliatus subsp. Richardsonii, are the most common plants of Harding Lake. This pteridophyte was found uniformly throughout the zone of major

hydrophyte colonization, while no specimens were discovered outside this zone. Collections were made at depths ranging from 25 to 250 centimeters. The plants were frequently found in areas of hard-packed sand, rock fragments and cobbles, from which other species were excluded. The plants were found less frequently in sand/silt and silt substrata.

This species occupied each of the six transects, the height of the plants ranging from 1 to 6 centimeters; their low profile is shown in Figure 5b. In transects 1, 2, 3 and 4 this species was the most common, growing in a continuous stand from near 10 meters offshore to depths ranging to 255 centimeters. Population densities for these four transects were high, frequently 100 percent cover. In transects 5 and 6, this species was uncommon, growing at very low or negligible biomass at depths of 35 to 175 centimeters.

The species was a rosette-former, the stem entirely reduced with a whorl of 10 to 30 fronds rising spike-like from the hardened base. Figure 4 depicts the typical growth form of these plants, with the base of the fronds at the sediment surface and an extensive system of once-branching roots. The root system was generally longer than the shoot system, even in hard-packed substrata. Vegetative reproduction was not observed in Isoetes muricata var. Braunii, although fragmented plants were seen occasionally. Androspores were numerous in the basal portions of the outer fronds. The new growth did not appear above the sediment surface until after July 1, at which time the previous year's frond growth had deteriorated.

Figure 5.--Physiognomy of hydrophyte species populations in Harding Lake: (a) Eleocharis acicularis, transect 1; (b) Isoetes muricata var. Braunii, transect 1; and (c) Potamogeton filiformis, transect 5.



Sparganium angustifolium Michx.
(Sparganium affine Schnizl.)

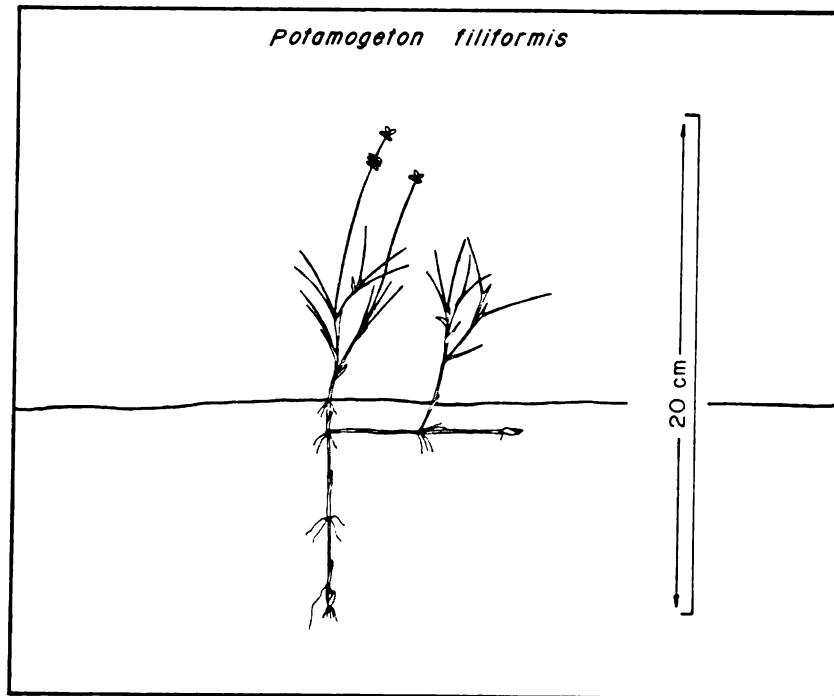
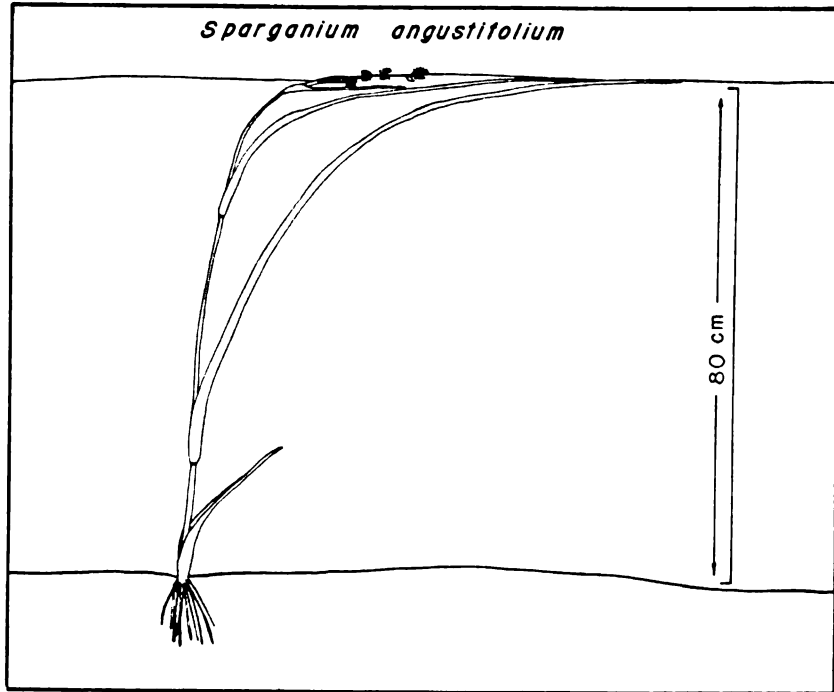
These plants were found in small, scattered colonies of 10 to 30 plants, in the zone of major hydrophyte colonization. Stands were sampled in transects 2, 3 and 4 in shallow water 6 to 80 centimeters deep. The substratum was sand to gravel in each case, with only a small amount of silt.

Each colony of Sparganium angustifolium had very distinct boundaries, with an even distribution throughout. The plants dominated the water surface with floating leaves, the only major Harding Lake taxon to do so (Potamogeton natans and Polygonum amphibium were also found, but were rare in the lake). In transect 2, the plants were 9 centimeters tall, just beginning growth at the time of sampling. Also present in this sample were Isoetes muricata var. Braunii and Potamogeton perfoliatus subsp. Richardsonii. In transects 3 and 4 S. angustifolium dominated the community from 5 to 20 meters from shore, occupying the water surface above individuals of I. muricata var. Braunii, P. filiformis, P. gramineus, P. perfoliatus subsp. Richardsonii, Eleocharis acicularis and Subularia aquatica.

S. angustifolium had an elongate stem which reached the water surface, bearing several flowers, usually two pistillate and three staminate. Several tape-like leaves emerged from the stem below the branching inflorescence to float on the water surface. Figure 6 shows a typical plant growing in 80 centimeters of water, with many simple roots seen below the sediment surface. The distinct colonial structure of these stands suggests vegetative reproduction,

Figure 6.--Growth habits of Sparganium angustifolium in Harding Lake, showing floating leaves and flowers, originating from a long, slender stem. Roots are many, unbranching; plants without rhizomal system.

Figure 7.--Growth habits of Potamogeton filiformis, depicting long, filiform leaves and seeds borne in one or two whorls, on elongated peduncles, with taproot extending downward to tuber. Secondary shoots are seen along rhizomal system.



although no stolons or rhizomes were observed. Seeds were abundant in these colonies near August 1.

Potamogeton filiformis Pers.

These plants were found scattered singly over most areas of Harding Lake. This is the only taxon found to inhabit large areas of the northern littoral portion of the lake where gravel rock fragments and cobbles formed the principal substrata. P. filiformis was collected also from transects 1, 3, 5 and 6, growing at depths from 25 to 185 centimeters, but usually less than 50 centimeters.

P. filiformis was a small plant, growing to a height of only 10 to 12 centimeters. The low profile of this species is shown in Figure 5c, where it is seen in transect 5 along a gradual slope, between the 42 and 110 centimeter depths. P. filiformis, along with Isoetes muricata var. Braunii, P. gramineus and Eleocharis acicularis, formed an understory of plants below P. perfoliatus subsp. Richardsonii in transect 5. In transect 3, P. filiformis formed an understory of plants below Sparganium angustifolium. These plants were tallest in their zone of occurrence in transects 1 and 6. There they grew alone or above I. muricata var. Braunii and E. acicularis.

Potamogeton filiformis had a branching stem with many filiform leaves. Flowers were borne in whorls on an elongated stalk. Figure 7 shows the long, delicate taproot extending as much as 10 centimeters into the sediment where a small tuber was borne. A few simple roots were found at each junction of the taproot and the rhizome system. While 10 to 20 seeds formed in each plant on one or two flowering stalks, the plants apparently perennated from the tuber.

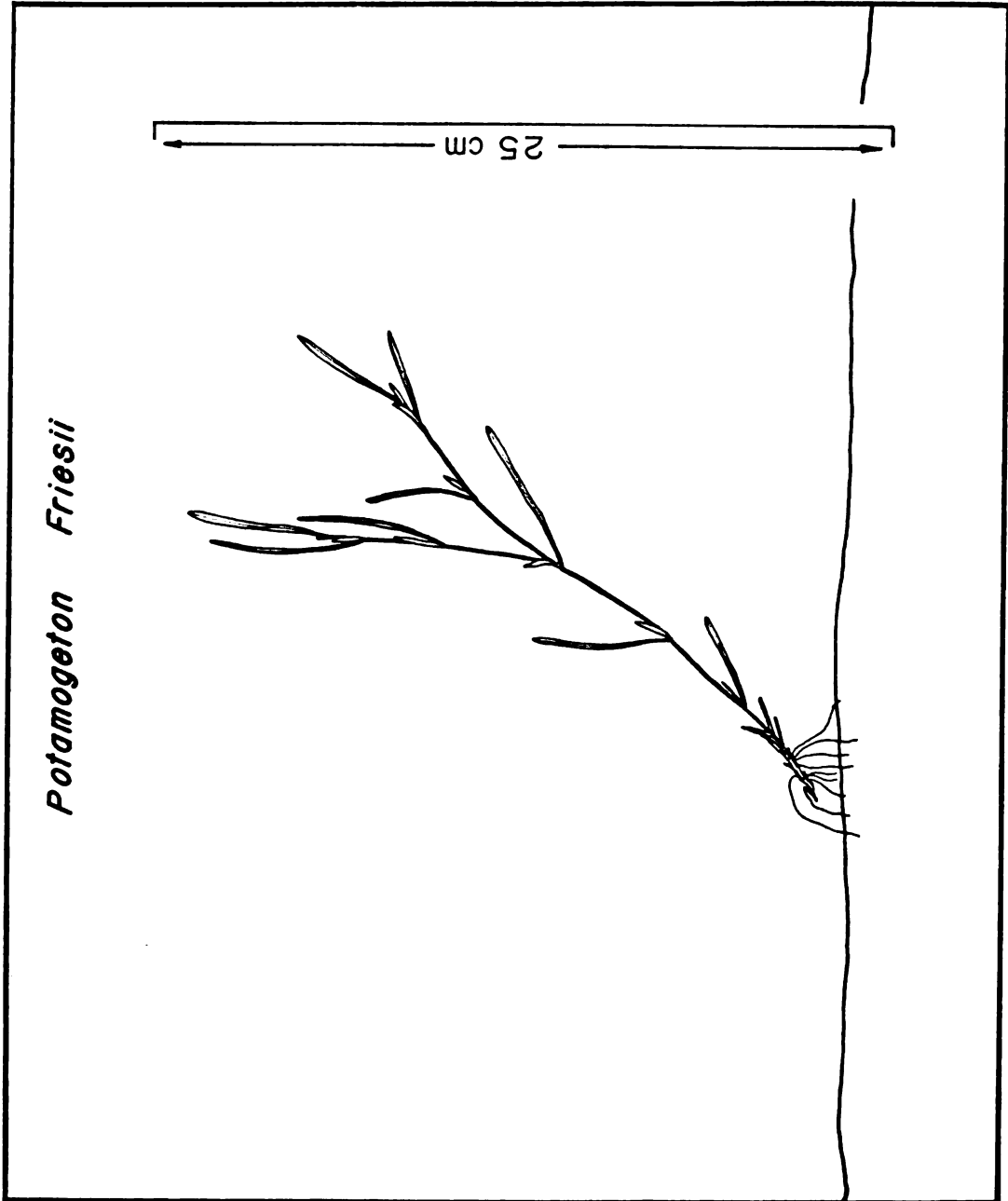
Germinating seeds were not observed, although the highly random distribution of these plants suggested reproduction by seeds.

Potamogeton Friesii Rupr.
(Potamogeton mucronatus Schrad.)

Potamogeton Friesii was uncommon in Harding Lake, seen only in transect 6 between the 350 and 420 centimeter depths. The plants were scattered about the sediment surface, rising to a height of 20 centimeters, but apparently still growing at the time of transect sampling. This species was associated with P. perfoliatus subsp. Richardsonii at the 350 centimeter depth, but was the only species observed between the 355 and 420 centimeter depths. The population was most dense at the 350 and 365 centimeter depths. It was negligible in the deeper samples.

This species appeared to be strictly vegetatively reproduced. Figure 8 shows a shoot system arising from a fragment of the previous year's shoot, presumably a winter bud. Plant fragments floated along the substratum until roots were formed in the basal nodes of the winter bud. As the shoot growth began, the roots reached the sediments, anchoring the plants against the buoyancy of the rapidly growing shoot system. Plants were not observed to flower by August 15, when water temperatures began a rapid decrease, so it is probable that winter buds are the sole means of reproduction for Harding Lake populations of P. Friesii.

Figure 8.--Growth habits of Potamogeton Friesii in Harding Lake,
showing root and shoot extension from winter bud
above substratum.



Potamogeton gramineus L.
(Potamogeton heterophyllus of authors)

Two forms of Potamogeton gramineus, described below, were observed in Harding Lake. A shallow-water form was restricted to a small area of silt deposition on the northeast shoreline of the lake as noted in Figure 2. A deep-water form was found commonly throughout the zone of major hydrophyte colonization, and was represented in transects 2, 3, 4 and 5. Figure 9a depicts the physiognomy of this species in transect 5. These deep-water plants were found at depths from 18 to 120 centimeters in sand/silt substrata, while the shallow-water plants were located in silt areas with water 6 centimeters, or less, deep.

This species was quite variable in form in Harding Lake. It has been noted to hybridize with P. perfoliatus subsp. Richardsonii and P. praelongus (Hulten, 1968). The deepwater form was found completely submersed at the 18 to 120 centimeter depth levels. Internodal distances were equal (+) to the leaf length, and fruiting occurred entirely below the water surface. This is shown in Figure 10. The shallow-water form is depicted in Figure 11. Internodal distances were reduced and most leaves floated at the surface. Flowers were not collected from the shallow-water populations. In both forms, rhizome systems with secondary shoots were present, while a taproot extended into the sediment to a tuber.

Potamogeton natans L.

Only one individual of this species was observed in Harding Lake during the present study. The plant was located in the northeast

Figure 9.--Physiognomy of hydrophyte species populations in Harding Lake: (a) Potamogeton gramineus, transect 5; (b) Potamogeton perfoliatus subsp. Richardsonii, transect 5, (c) Potamogeton praelongus, transect 5.

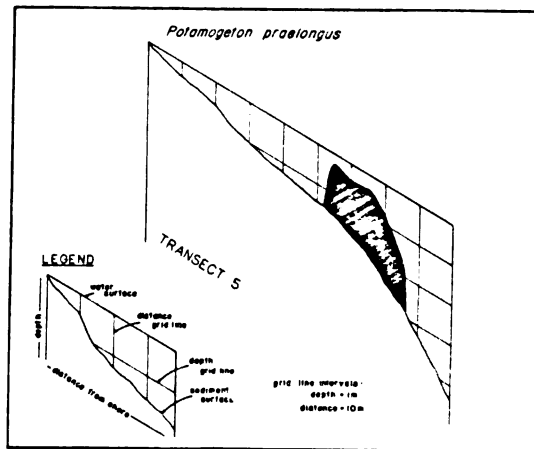
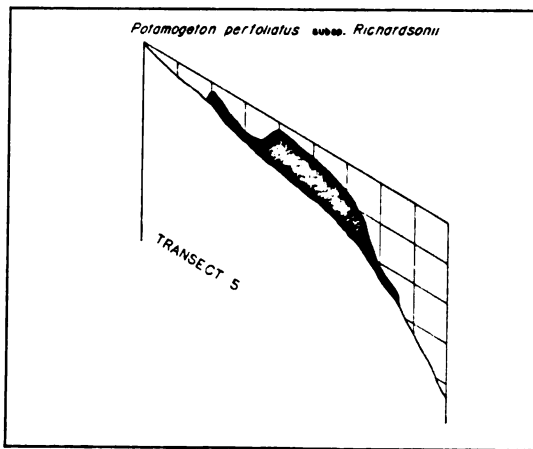
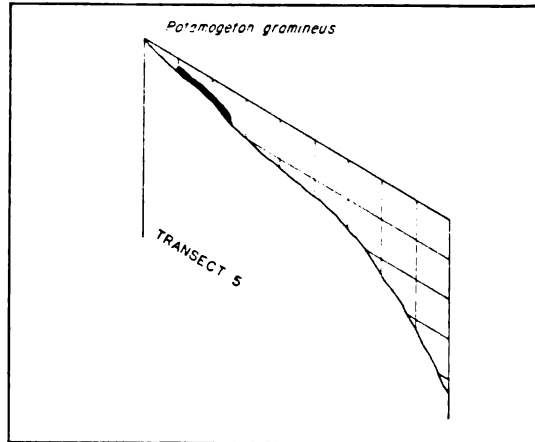


Figure 10.--Growth habits of Potamogeton gramineus, deep-water form, in Harding Lake, showing spike of seeds on elongate peduncle, numerous submersed leaves and rhizomal system with taproot extending downward to tuber.

Potamogeton gramineus
(deep-water form)

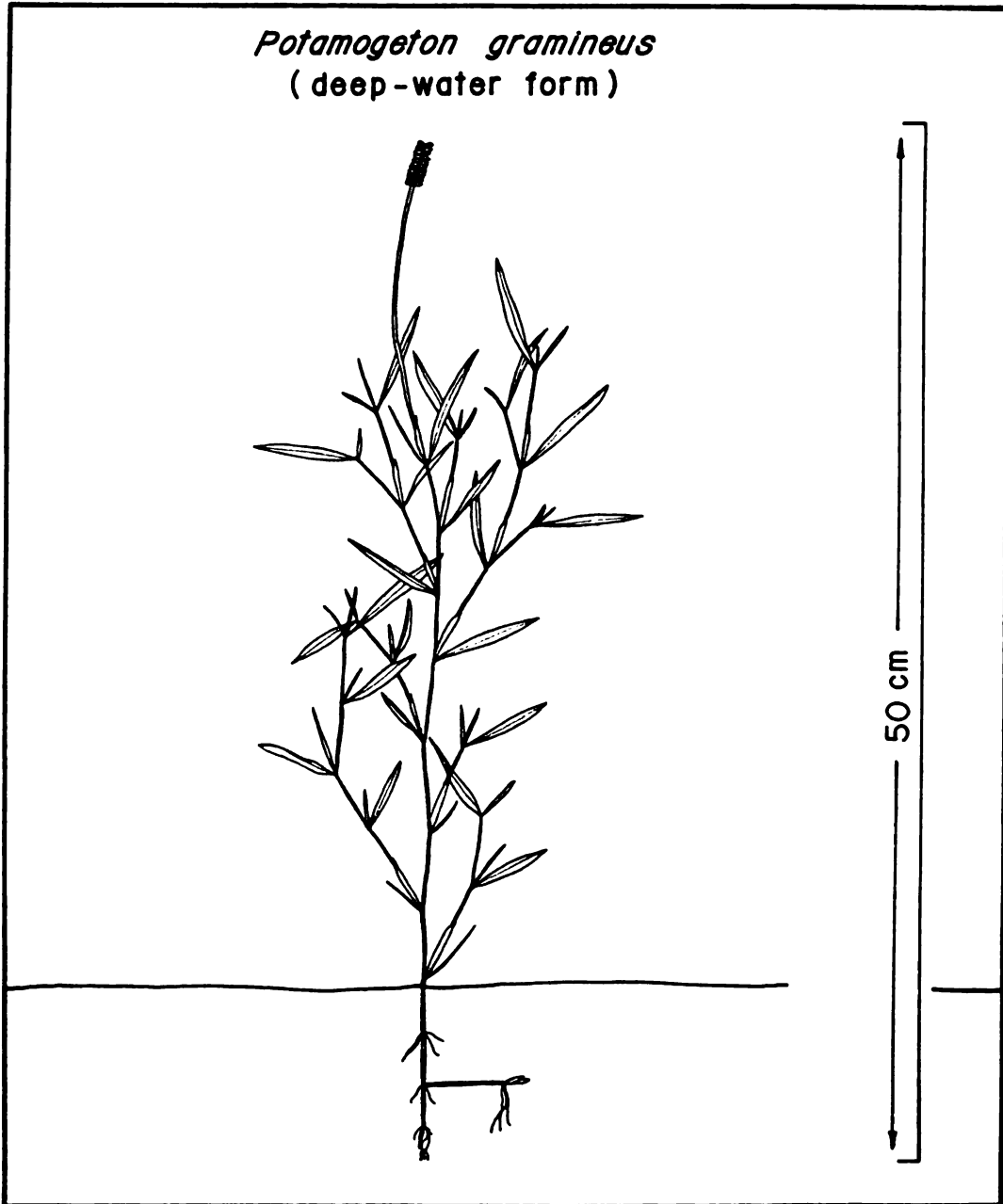
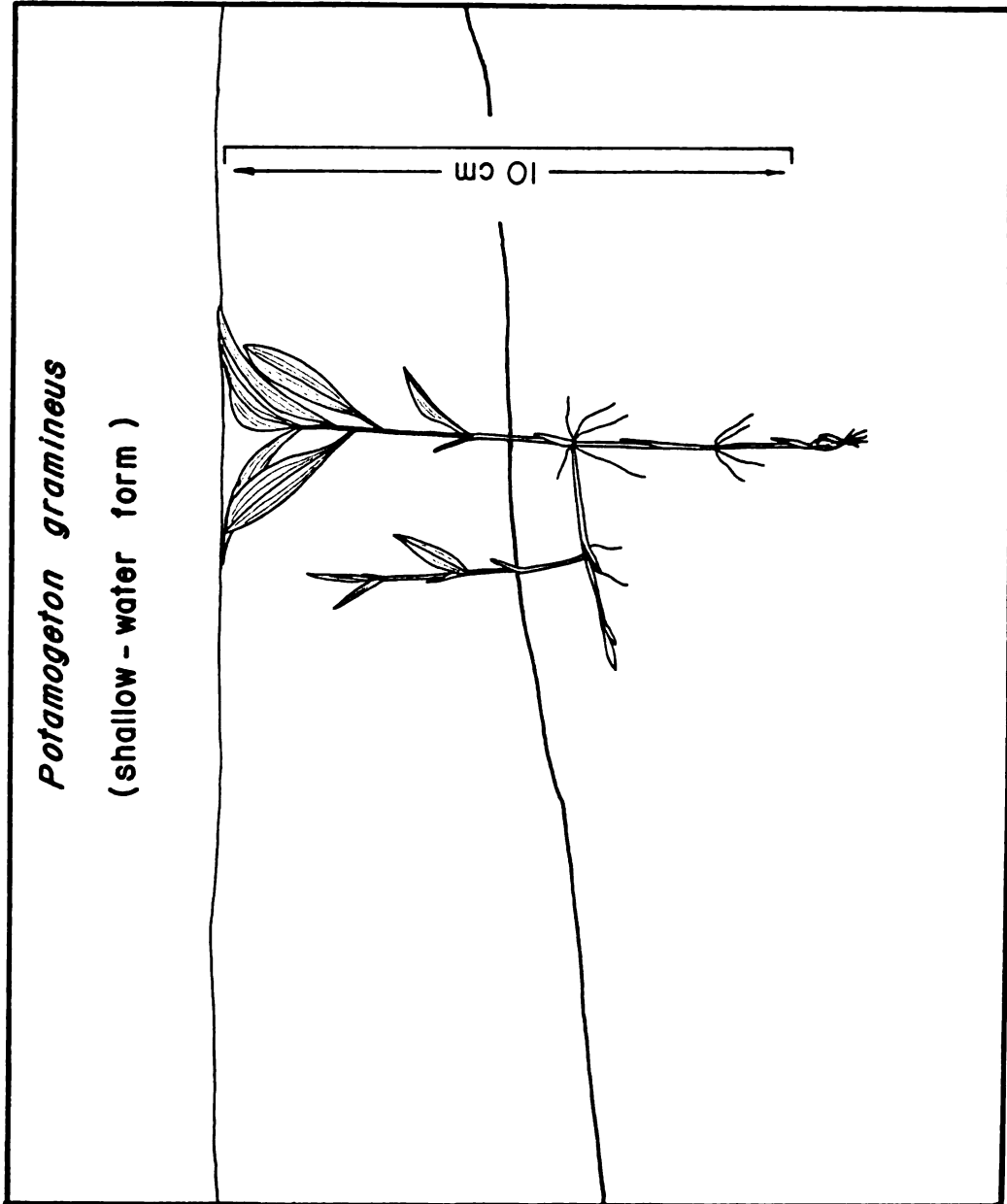


Figure 11.--Growth habits of shallow-water form of Potamogeton
gramineus in Harding Lake, showing floating leaves,
rhizomat system and taproot extending downward to
tuber.



quadrant of the lake in a stand of Polygonum amphibium. It was in a deteriorated condition, with no flowers present.

Potamogeton perfoliatus subsp. Richardsonii
(Bennett) Hulten
(Potamogeton perfoliatus var. Richardsonii
Bennett; P. Richardsonii (Bennett) Rybd.)

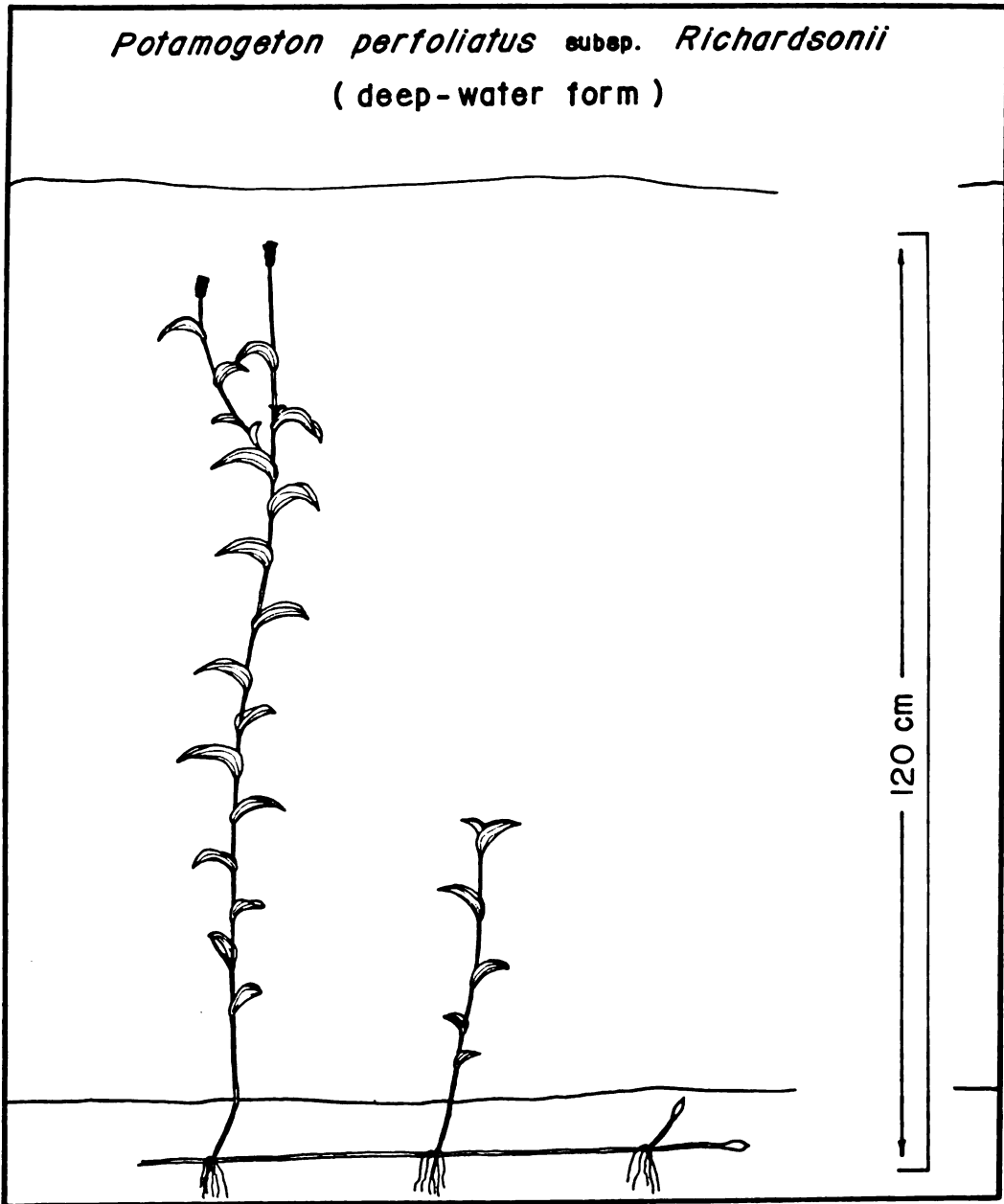
This was the most abundant species in Harding Lake, occurring in all transects. It grew in water 25 to 350 centimeters deep. As in P. gramineus, two forms were found. Only the deep-water forms were present in the transects. The shallow-water form was found in conjunction with similar forms of P. gramineus along the northeast shoreline of the lake. The deep-water form, while restricted to the zone of major hydrophyte colonization, was ubiquitous there. This uniform distribution occurred under varying conditions of substratum and depth.

P. perfoliatus subsp. Richardsonii was often dominant in height over a collection of understory species. Figure 9b shows the population profile of this species in transect 5. This was typical of all transects except transect 2, where only a small group of plants was found at the 120 centimeter depth.

As noted above, this species is known to hybridize with P. gramineus (Hulten 1968). The form of some individuals collected in Harding Lake suggest hybridization with P. praelongus, but this is not confirmed in the literature. The deep-water form, shown in Figure 12, was a tall plant, with an elongate stem reaching to just below the surface of the water. The stem frequently branched in its terminal portion, bearing one flower spike on each branch. Flowers

Figure 12.--Growth habits of Potamogeton perfoliatus subsp. Richardsonii, deep-water form, in Harding Lake, depicting branching shoots with flower spikes and extensive rhizome and secondary shoot system.

Potamogeton perfoliatus subsp. *Richardsonii*
(deep-water form)



were borne below the water surface in all specimens. The shallow-water form, shown in Figure 13, had an unbranched stem with internodes reduced. Flower spikes were borne above the water surface. In both forms, the rhizomes were very fibrous. Roots and secondary shoots were numerous. Reproduction by seeds and perennating portions of the rhizome was likely.

Potamogeton praelongus Wulf.

This species was found in dense, but scattered, monospecific stands in the littoral area of Harding Lake. Major stands were found in the northeast and northwest quadrants of the lake and on the gravel point of land along the south shore of the lake. These locations are noted in Figure 2. Only small clusters were found in the zone of major hydrophyte colonization. Plants were normally found in 250 to 420 centimeter depths, in zones of heavy siltation. Of the transects, only transect 5 was occupied by P. praelongus. The population of transect 5, shown in Figure 9c, was atypical because of the shallow distribution (150 to 250 centimeters) and the co-dominance of P. perfoliatus subsp. Richardsonii.

This species exhibited the most extensive rhizome system of any of the Harding Lake taxa; many fertile shoots were interconnected. Figure 14 shows a portion of the massive shoot/rhizome system with branching stems bearing flower spikes below the water surface, and large rhizomes 10 to 15 centimeters below the sediment surface. Plants extended to the surface from as much as 420 centimeter depth. While seeds were present, the perennation of the rhizome system was likely the mode of reproduction in these plants.

Figure 13.--Growth habits of Potamogeton perfoliatus subsp. Richardsonii, shallow-water form, in Harding Lake, showing compacted stem, spike of seeds and extensive rhizome and secondary stem system.

Potamogeton perfoliatus subsp. *Richardsonii*
(shallow - water form)

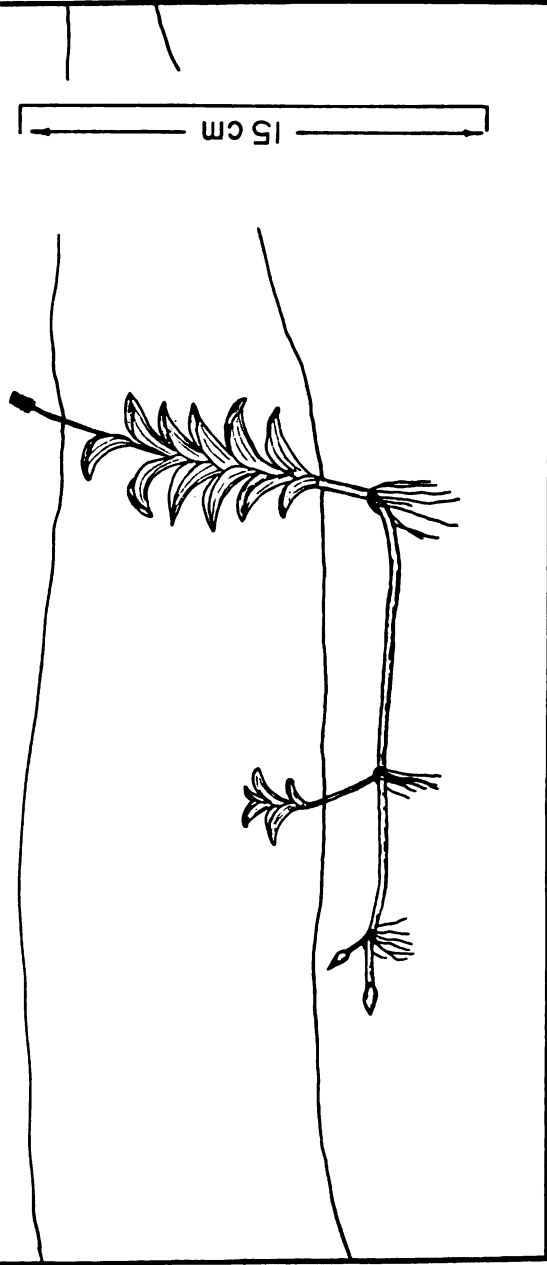
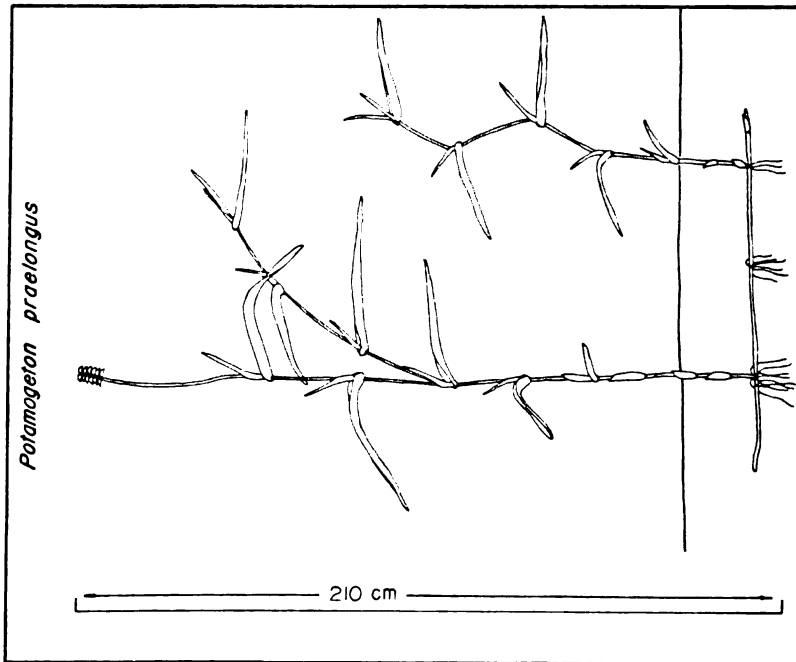
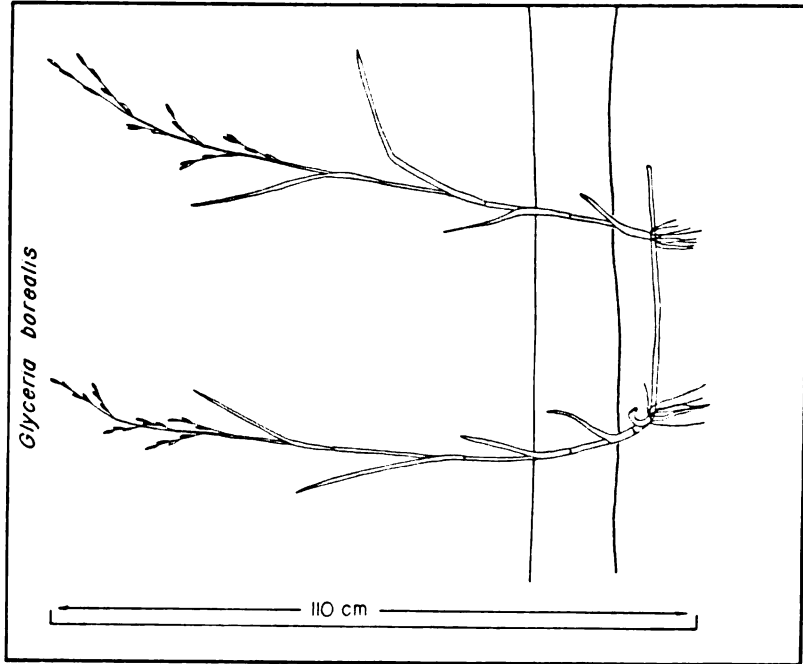


Figure 14.--Growth habits of Potamogeton praelongus in Harding Lake, showing large leaves on branching stem, flower spikes below the water surface and strong rhizomal system with secondary shoots.

Figure 15.--Growth habits of Glyceria borealis in Harding Lake, depicting rhizomal system development with mature spikes rising above the water surface.



Glyceria borealis (Nash) Batchelder)
(Panicularia borealis Nash)

This species was found only in transect 1 from shore to the 25 centimeter depth. The plants were the only emergents found in the zone of major hydrophyte colonization. The shoots grew to a total height of 100 centimeters from the sediments. The plants dominated an understory community of Isoetes muricata var. Braunii and Potamogeton filiformis. Shoots of Glyceria borealis were interconnected by small rhizomes, as shown in Figure 15. Achenes were borne in slender heads on shoots bearing 2 to 4 leaves.

Eleocharis acicularis (L.) Roem & Schult.
(Scirpus acicularis L.)

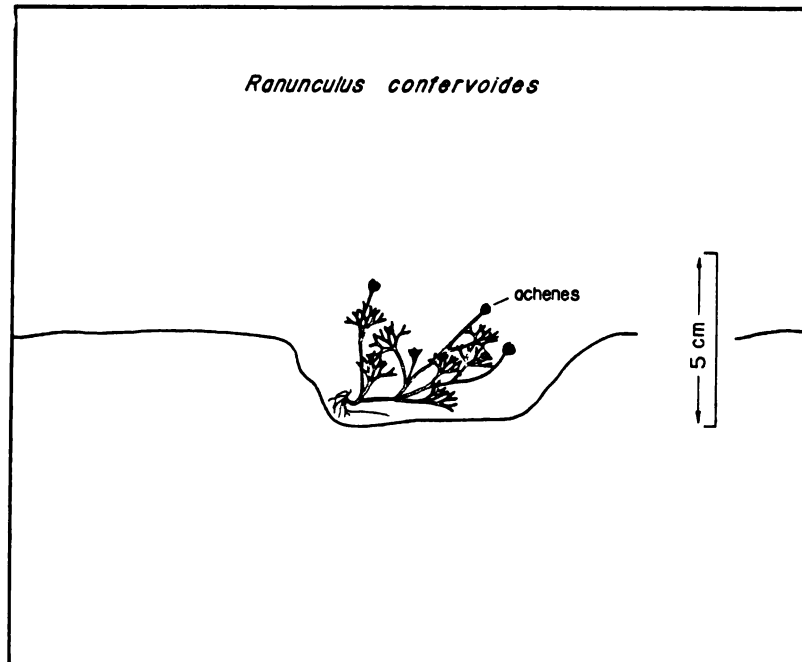
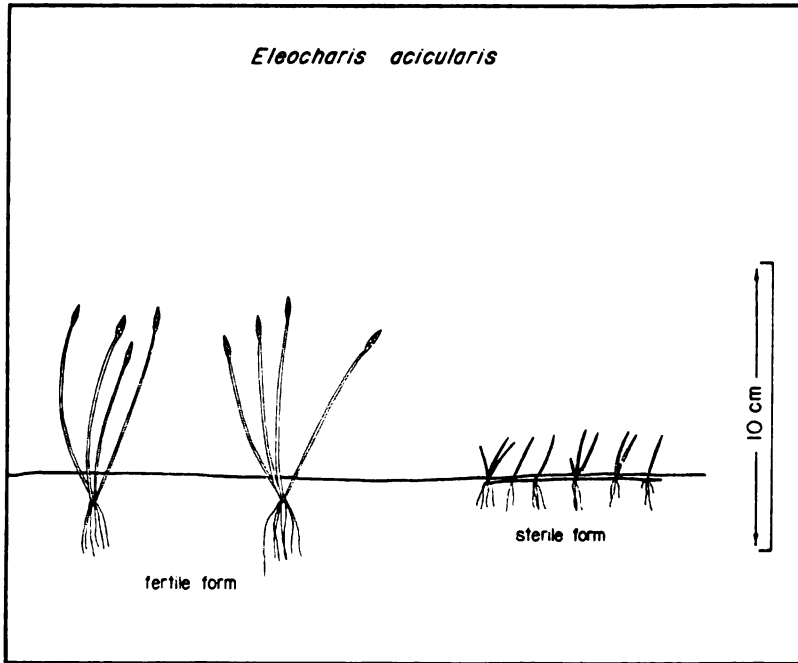
Two forms of Eleocharis acicularis were found in Harding Lake. Both were very common. A sterile form was found in the wave-washed areas of the zone of major hydrophyte colonization, while a fertile form was found lakeward from the former, to depths of 120 centimeters.

The sterile form of this species was present in very dense mats of interwoven shoot/rhizome systems with Subularia aquatica. These never extended more than one or two meters from the shoreline, usually in areas washed by waves. Some stands were emergent, but this habit was likely due to low water levels. These plants grew to less than 3 centimeters, as shown in Figure 16.

The fertile form of this species, seen in transects 1, 2, 4 and 5, was found in sparse stands to 120 centimeter depths. Its physiognomy is shown in Figure 5a. These plants grew in tufts of 5

Figure 16.--Growth habits of Eleocharis acicularis in Harding Lake, depicting fertile form growing in isolated tufts and the much smaller sterile form, growing along an extensive rhizomal system.

Figure 17.--Growth habits of Ranunculus confervoides in Harding Lake, showing small tuft of plant resting in substratum depression. Small roots are present, but do not penetrate sediment surface. Seeds are borne in achenes.



to 20 shoots, with terminal spikelets as shown in Figure 16.

Plants grew to 8 to 10 centimeters above the sediment surface.

Eleocharis palustris (L.)

These plants were uncommon in Harding Lake, found in a sparse stand in the northern area of the lake at the 2 to 10 centimeter depths. The location is noted in Figure 3. Individuals reached heights of about 80 centimeters from a short, buried stem segment. Terminal spikelets were present but the reproductive mode is unknown.

Polygonum amphibium (L.)

This species was found in a small colony in the northern zone of the lake. The location is shown in Figure 3. Plants grew in water 20 to 50 centimeters deep, with leaves and flowers floating at the surface. Plants were interconnected by rhizomes.

Ranunculus confervoides (E. Fries) E. Fries
(Batrachium confervoides E. Fries)

These plants were first observed in late June, lying in small pockets in the substratum. The latter were formed by groundwater flow and were filled with milky-white water. These occurrences were limited to transects 3 and 6. In transect 3 at 195 centimeter depth, the plants grew below individuals of Potamogeton perfoliatus subsp. Richardsonii and Myriophyllum sp., as was Isoetes muricata var. Braunii. In transect 6, the plants occurred alone at the 150 centimeter depth.

Small tufts of this plant were also found rolling and drifting along the sediment surface. While roots were present, as shown

in Figure 17, they were never seen to penetrate deeply into the substratum. Many seeds were present.

Subularia aquatica L.

This very small plant was distributed similarly to the sterile form of Eleocharis acicularis; they were usually in co-occurrence. The species, while common throughout the wave-washed areas of the lake, was only found in transect 4, between 16 and 18 centimeter depths.

The plants were very short in stature, always sparsely inhabiting E. acicularis mats. The tallest specimens were 2 to 3 centimeters above the sediment surface, slightly taller than the surrounding E. acicularis. In its occurrence in transect 4, S. aquatica was in an understory community below Sparganium angustifolium, along with E. acicularis and Potamogeton gramineus.

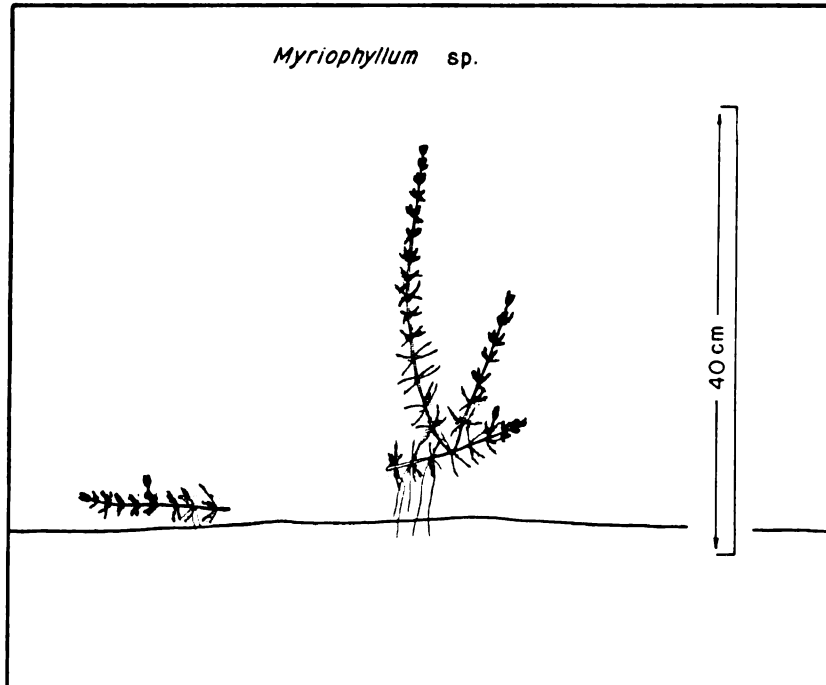
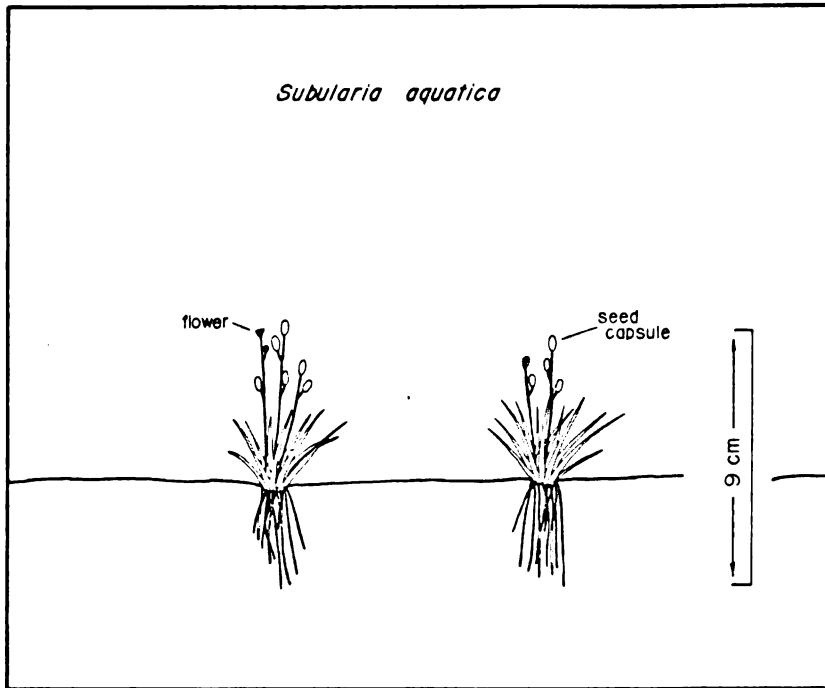
Subularia aquatica was a rosette-former, the leaves whorled around a reduced stem and the flowers borne on a branching inflorescence (Figure 18). Seed pods were numerous, all below the water surface. Hulten (1968) notes that the flowers are cleistogamous in submersed individuals.

Myriophyllum sp.

This species was found only in transect 3, from 170 to 340 centimeter depths. Plants grew to 20 to 60 centimeters tall and were co-dominant with Potamogeton perfoliatus subsp. Richardsonii in the deep-water portions of transect 3. The understory species included Isoetes muricata var. Braunii and Ranunculus confervoides.

Figure 18.--Growth habits of Subularia aquatica in Harding Lake, showing whorl of leaves growing from reduced stem, tuft of unbranching roots and flowers and seed capsules growing on long peduncles.

Figure 19.--Growth habits of Myriophyllum sp. in Harding Lake, showing new roots and shoots growing from previous year's winter buds. Roots can be seen to penetrate sediment surface.



Flowering specimens were not found. The vegetative material suggests M. exalbescens Fern. All growth was from winter buds. These were about 10 centimeters long and were scattered about the surface of the sediment in June and early July. Growth began in late July and was rapid in early August; it is doubtful they reached flowering as water temperatures were likely limiting growth after mid-August. Roots formed at the nodes of the basal portion of the buds (Figure 19), while shoots extended from the distal portions of the buds.

DISCUSSION

Descriptions of the biogeographical ecologies of vascular hydrophyte species over their entire ranges are notably absent from the literature. However, studies of chemical water quality conditions show that submersed vascular hydrophyte species are tolerant of a wide range of freshwater environments. Moyle (1945), Olsen (1950a,b) and Seddon (1967, 1972) have observed the relation of vascular hydrophyte species' occurrences to chemical water quality variables such as pH, alkalinity, hardness and conductivity. In each study, many lakes were sampled over geographically limited areas. Their results show that most species occurred in widely varying chemical conditions. This leads to the expectation that vascular hydrophyte species are largely indifferent to water quality conditions within the freshwater range.

Studies considering the distributions of vascular hydrophyte species within lakes present a complex view of species' ecologies. These investigations center on the physical habitat variables and their relation to plant growth form. For example, wave action has been cited by Pearsall (1920), Wilson (1935, 1937, 1941) and Spence (1967) as a principle variable controlling shallow-water plant colonization. Plants inhabiting this zone are subject to mechanical action of the water, scouring by water-carried sand and silt particles and a lack of organic matter in the substratum. Most areas

of the Harding Lake shoreline were subjected to strong wave action. In areas of unabated wave action, dense mats of Eleocharis acicularis and Subularia aquatica were found. Wave damage in these plants with short, fibrous, filiform leaves was minimal. The extensive rhizome system of E. acicularis provided stability for the mat community (see Figure 16). An offshore gravel bar in the northeast quadrant of the lake protected several less wave-resistant species. E. palustris, Polygonum amphibium and Potamogeton natans, each with a vegetative form susceptible to wave damage, had their sole occurrences in this area.

The same authors point out that wave-generated currents carry small soil particles lakeward from the shore and shallow-water zones. In Harding Lake the siltation was quite variable, depending upon upland terrain. Siltation was greatest in the southern zone with high deposition beginning near the 4-meter depth contour where the bottom slopes increase sharply. The northern area of the lake had no siltation and the substratum was composed of sand and gravel from the shore to the 2-meter depth contour and rock fragments and cobbles lakeward to beyond the 6-meter depth contour.

Most vascular hydrophyte populations of the lake were found shoreward of the zones of heaviest siltation. Potamogeton praelongus and P. perfoliatus subsp. Richardsonii were the only species of Harding Lake which were found in areas of heavy siltation. Isoetes muricata var. Braunii was the only species of Harding Lake consistently growing in silt-free areas. These observations concur with those of Wilson (1937). Based on the observations by Wilson (1937)

and of Harding Lake hydrophytes, the large-leaved Potamogeton spp. appear to be the most siltation-tolerant submersed hydrophytes. The small rosette and filiform-leaved plants seem to be the least siltation-tolerant.

Thermal limitations to growth of submersed hydrophyte populations in Harding Lake may have been significant. The winter's ice rapidly diminished in the last week of May. The lake was roughly isothermal at 4° Celsius on May 31. Stable stratification was established by June 20, with surface temperatures of 15° Celsius. On this date, the 4° isotherm was near the 4-meter depth. By July 19 and through the second week of August, the 10° isotherm was near the 8-meter depth. Surface temperatures increased during this period from 15° to 19° Celsius. Internal seiches carried near 4° water into the shallow littoral areas on several occasions during the six-week period beginning on July 1. Aquatic plant growth usually occurs at temperatures above 10° Celsius, but the effect of the short, periodic exposures to very cold temperatures is unknown.

The timing of growth events of the plant populations suggests varying thermal tolerances among the species. Some Potamogeton praelongus stands flowered by the third week of June, the earliest observed in the lake. Similar early season growth patterns have been observed in Michigan populations of P. praelongus (McNabb, 1976). The latest development was observed in Myriophyllum sp. and P. Friesii populations which did not begin growth until the last week of July. Prior to this time, dormant winter buds of both had been observed on the substratum surface. Since light energy levels were decreasing

at the time growth began in most Harding Lake taxa, light energy inputs do not seem likely to have controlled the timing of growth patterns.

Light levels in Harding Lake may, however, have limited vascular hydrophyte distributions and growth rates. Water clarity in the lake was very high with one percent of the light incident to the surface reaching the 16-meter depth (LaPerriere, et al., 1975). The deepest penetration of vascular hydrophytes recorded in 1974 was Potamogeton praelongus at 4.2 meters. Observations cited by Hutchinson (1975) indicate vascular hydrophyte penetration to as deep as 11 meters in lakes of equal or lower transparency. The disparity between observations on Harding Lake and lakes of lower latitude points out the inadequacy of water transparency data as the lone factor in explaining within-lake plant distributions.

Since the rate of solar energy input to any depth depends on the angle of incidence of the light, the highest instantaneous rates are found in the tropics. The highest daily total energy inputs to lakes occur in the mid-temperate latitudes where the day-length is longer. In arctic latitudes the low path of the sun through the sky causes low instantaneous rates and low daily total rates of energy inputs to lakes. This leads to the expectation that zonation patterns of submersed hydrophyte populations may be shifted to increasingly shallower depths with increasing latitude above the tropics. (This concept is developed more completely in Appendix I.) But light and temperature regimes both appear to have

influenced the plant distributions and their effects can only be separated experimentally.

Scientists attempting to describe the biogeographical ecologies of vascular hydrophyte species face a remarkably difficult question. To catalogue species occurrences and corresponding habitat conditions has been of only limited value. It is clearly true that at least one dissemule of each species was deposited in Harding Lake at some time prior to this study. It is also true that the lake provided a suitable habitat for its hydrophyte flora. It is not predictable, however, that a limnologically similar lake in a neighboring watershed would harbor the same species. In fact, the studies cited above collectively demonstrate that a lake basin with particular chemical and physical properties is susceptible to colonization by a large number of species and that of these only a fraction will be inhabitants at any one time. Since the migrations of plants depend on largely random events, the prediction of the flora of a lake basin is not likely. However, it should be possible to predict the physiognomy of the plant communities based on knowledge of the interrelation of plant growth forms and physical habitat constraints of the basin.

LITERATURE CITED

LITERATURE CITED

- Blackwell, M. J. 1965. Surficial geology and geomorphology of the Harding Lake area, Big Delta quadrangle, Alaska. Unpublished M.S. thesis. Fairbanks, Alaska, Library, University of Alaska. 91 pp.
- Fassett, N. C. 1966. A Manual of Aquatic Plants. The University of Wisconsin Press, Madison, Wisconsin. 405+ ix pp.
- Hulten, E. 1968. Flora of Alaska and Neighboring Territories. Stanford University Press, Stanford, California. 1008+ xxii pp.
- Hutchinson, G. E. 1975. A Treatise on Limnology. Vol. III. Limnological Botany. Wiley Interscience, New York. 660+ x pp.
- LaPerriere, J. D., L. A. Casper and F. C. Payne. 1975. Difficulties in assigning a trophic state to a deep subarctic lake. *Verh. Internat. Verein. Limnol.* 19:480-486.
- McNabb, C. D., Jr. 1976. Personal communication.
- Moyle, J. B. 1945. Some chemical factors influencing the distribution of aquatic plants in Minnesota. *Amer. Midl. Nat.* 34:402-420.
- Olsen, S. 1950a. Aquatic plants and hydrospheric factors. I. Aquatic plants in S.W. Jutland, Denmark. *Svensk Botanisk Tidskrift* 44:1-34.
- _____. 1950b. Aquatic plants and hydrospheric factors. II. The hydrospheric types. *Svensk Botanisk Tidskrift* 44: 332-373.
- Pearsall, W. H. 1920. The aquatic vegetation of the English Lakes. *J. Ecol.* 6:75-83.
- Seddon, B. 1967. The lacustrine environment in relation to macroscopic vegetation. In: Quaternary Paleoecology (E. J. Cushing and H. E. Wright, eds.), pp. 205-215. Yale University Press, New Haven, Connecticut.

Seddon, B. 1972. Aquatic macrophytes as limnological indicators. *Freshwater Biol.* 2:107-130.

Spence, D. H. N. 1967. Factors controlling the distribution of freshwater macrophytes with particular reference to the lochs of Scotland. *J. Ecol.* 55:147-170.

Wetzel, R. G. 1975. Limnology. W. B. Saunders, Philadelphia, Pennsylvania. 743+ ix pp.

Wilson, L. R. 1935. Lake development and plant succession in Vilas Co., Wisconsin. *Ecol. Monog.* 5:207-247.

_____. 1937. A quantitative and ecological study of the larger aquatic plants of Sweeny Lake, Oneida Co., Wisconsin. *Torrey Bot. Club, Bull.* 64:199-208.

_____. 1941. The larger aquatic vegetation of Trout Lake, Vilas Co., Wisconsin. *Wis. Acad. Sci., Arts and Letters, Trans.* 33:135-146.

APPENDICES

APPENDIX I

CALCULATION OF THE POTENTIAL RATES OF SOLAR
ENERGY INPUTS TO AQUATIC SYSTEMS AS
INFLUENCED BY LATITUDE

ABSTRACT

A model is presented for the calculation of maximum potential solar irradiance inputs to aquatic systems. The zenith angle of the sun is calculated from latitude, declination and hour-angle values. The hourly zenith angles are utilized in calculation of atmospheric attenuation, reflection at the air-water interface and light path length and attenuation to a specified depth of water. Sample calculations at the summer solstice show that daily total irradiance to any depth decreases above mid-temperate latitudes. Daily total irradiance to depths greater than 4 meters decreases above tropical latitudes.

INTRODUCTION

Arctic and subarctic aquatic productivity is often thought to be less limited by solar energy inputs during the ice-free season than similar bodies of water in the temperate latitudes. While daily total solar energy incident to the earth's upper atmosphere increases with increasing latitude during the summer months, the sun's path becomes lower in the sky. Atmospheric attenuation, reflection at the air-water interface and the light path length to any depth are increased, so the peak rates of solar energy inputs to aquatic systems diminish with increasing latitude. The influences of these primary variables are calculable through basic physical "laws." When taken simultaneously into account they yield approximations of the theoretical maximum light energy reaching a specified depth of water, for any length of time during the ice-free period.

METHODS

The sun's nuclear furnace bombards the earth with electromagnetic radiation spanning a broad spectrum of wavelengths. The largest component is the light energy; the photosynthetically active 400-700 nm waveband is of the greatest interest to ecologists. Figure A1 shows the distribution of solar energy inputs from the ultraviolet (high frequency) to the infra-red (low-frequency) regions of the spectrum. The rate of energy input for any waveband is the product of the bandwidth (cm^{-1}) and the mean rate of energy input per wave-number in that band ($\text{cal}/\text{cm}^2/\text{min}/\text{cm}^{-1}$). The light energy in any waveband is diminished along its path to the aquatic system by absorption, scattering and reflection.

All aspects of the calculation of light reception at the earth's surface depend upon the path of the sun through the sky. Three variables, shown in Figure A2, are used in the calculation of the sun's path. This figure, called the celestial sphere, is the astronomer's basis for mapping the heavens from earth. The sphere is an imaginary surface, the projection of our earthbound frame of reference onto the sky. As this discussion centers on the motion of the sun, the radius of the sphere will be set as the distance from the earth to the sun at whatever time is being considered. The two celestial poles are the projection of the earth's poles onto the celestial sphere. Thus, the celestial sphere appears to earthbound

Figure A1.--Solar spectral irradiance incident to a surface perpendicular to the path of the light at the top of the earth's atmosphere (redrawn from Gates, 1962).

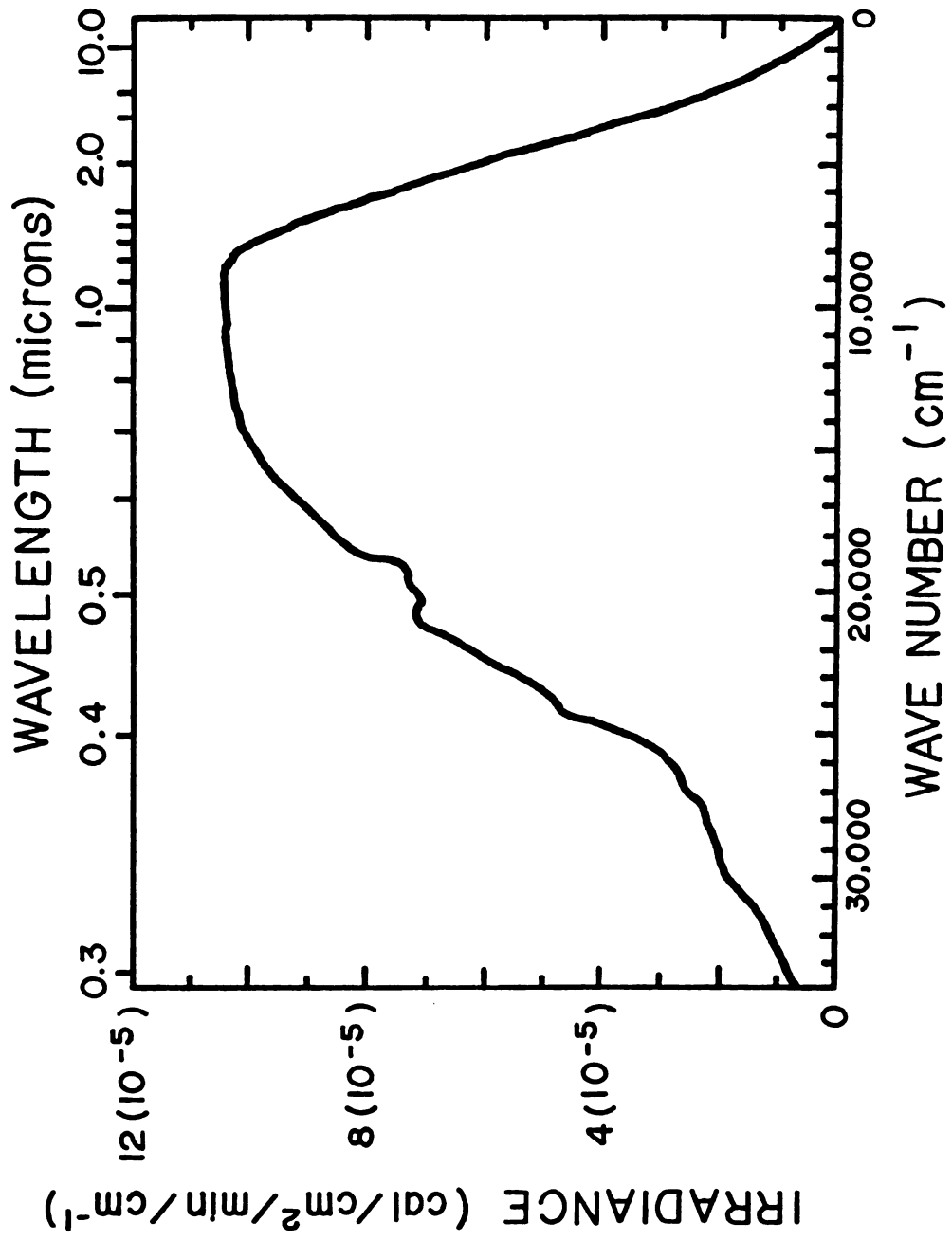
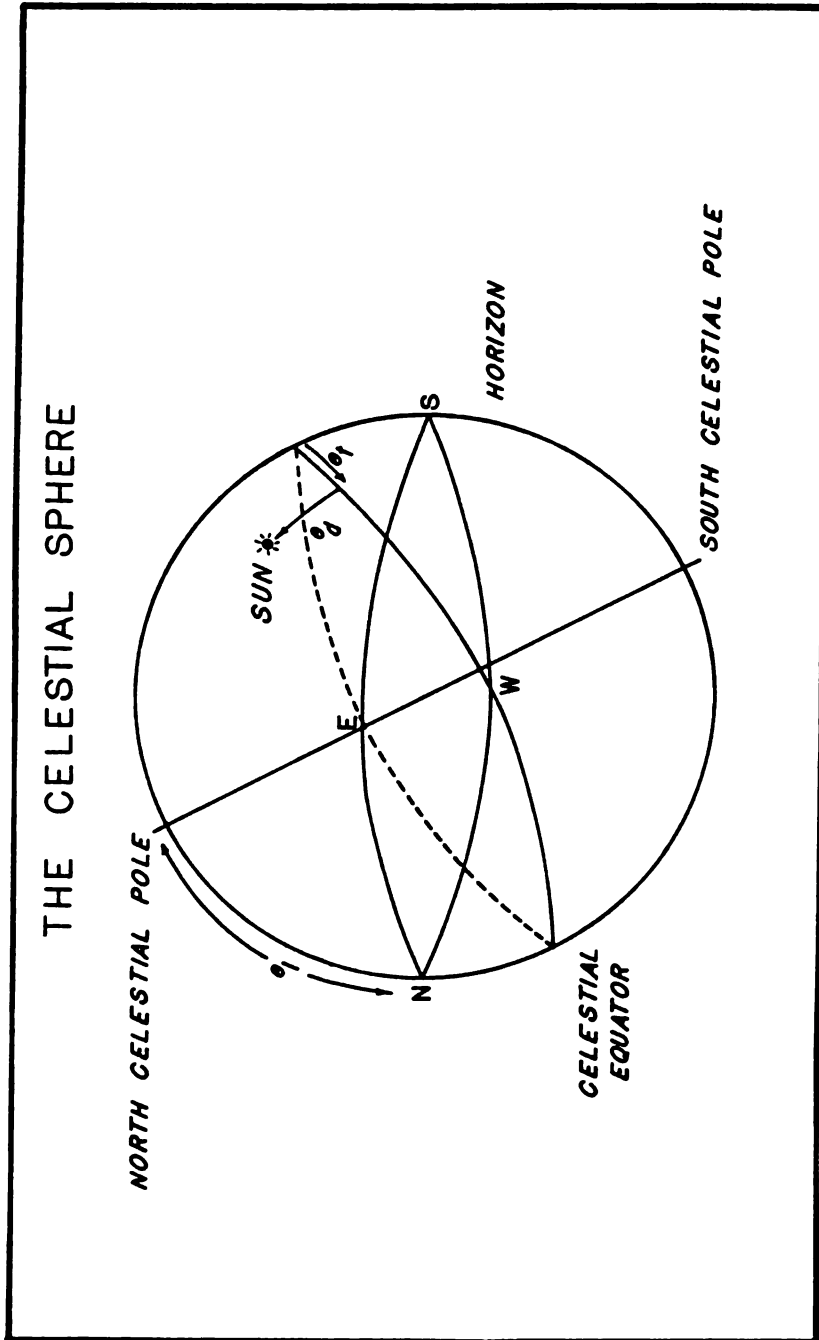


Figure A2.--The celestial sphere, relating variables necessary for the calculation of the sun's path through the sky.



observers to rotate about the celestial poles. The celestial axis is the line through the two poles, the projection of the earth's axis through space. The celestial equator is the projection of the earth's equator onto the celestial sphere. As seen in Figure A2, the celestial axis is perpendicular to the plane of the celestial equator.

The celestial sphere appears to rotate around our position on earth once every 24 hours due to the earth's rotation within the imaginary celestial sphere. This continual rotation yields the first variable to be considered in calculating the sun's path, the hour-angle, or θ_t . Since the earth rotates 360° in 24 hours, a movement of 15° equals one hour. Solar noon is set as the zero-angle, thus 15° is 1300 hours, 30° is 1400 hours, etc.

Throughout the year, the sun's latitude on the celestial sphere is continually changing, because the earth's axis is tilted 23.5° away from the perpendicular to its orbital plane. So seasonal changes in the latitude of the sun provide the second variable, the declination, or θ_d . In Figure A2, the sun is approximately 23.5° above the equator, so the northern hemisphere is receiving its longest day of the year, while the southern hemisphere is experiencing its shortest day of the year. Declination values are widely published, and are shown for every 3rd day of the year in Table A1.

The last variable needed is the observer's latitude, θ_l . Figure A2 illustrates the latitude by showing the projection of the observer's horizon onto the celestial sphere. As the observer's latitude approaches 90° , the observer's horizon coincides with the

TABLE A-1.--The sun's declination throughout the year (degrees).

Date	Decl.	Date	Decl.	Date	Decl.
Jan 1	-23.08	May 3	15.65	Sep 3	7.59
4	-22.82	6	16.51	6	6.48
7	-22.50	9	17.33	9	5.35
10	-22.10	12	18.11	12	4.22
13	-21.65	15	18.84	15	8.07
16	-21.13	18	19.53	18	1.91
19	-20.55	21	20.17	21	0.74
22	-19.92	24	20.75	24	-0.43
25	-19.22	27	21.28	27	-1.60
28	-18.47	30	21.76	30	-2.76
31	-17.67	Jun 2	22.18	Oct 3	-3.93
Feb 3	-16.83	5	22.54	6	-5.08
6	-15.93	8	22.84	9	-6.23
9	-15.00	11	23.08	12	-7.36
12	-14.03	14	23.26	15	-8.48
15	-13.03	17	23.38	18	-9.58
18	-12.00	20	23.44	21	-10.66
21	-10.93	23	23.43	24	-11.72
24	-9.86	26	23.36	27	-12.75
27	-9.75	29	23.24	30	-13.75
Mar 1	-7.62	Jul 2	22.18	Nov 2	-14.72
4	-6.57	5	22.80	5	-15.65
7	-5.31	8	22.49	8	-16.54
10	-4.14	11	22.12	11	-17.40
13	-2.96	14	21.70	14	-18.20
16	-1.78	17	21.22	17	-18.96
19	-0.59	20	20.68	20	-19.67
22	0.60	23	20.10	23	-20.32
25	1.78	26	19.46	26	-20.92
28	2.95	29	18.77	29	-21.46
31	4.12	Aug 1	18.04	Dec 2	-21.94
Apr 3	5.38	4	17.27	5	-22.36
6	6.42	7	16.45	8	-22.71
9	7.54	10	15.59	11	-22.99
12	8.65	13	14.70	14	-23.21
15	9.73	16	13.77	17	-23.35
18	10.79	19	12.81	20	-23.43
21	11.83	22	11.82	23	-23.43
24	12.83	25	10.79	26	-23.37
27	13.81	28	9.75	29	-23.23
30	14.74	31	8.68		

celestial equator. In fact, an observer at the earth's north pole, on the day illustrated in Figure A2, would see the sun trace a path all the way around the sky, always 23.5° above the horizon. Notice here that at the pole the sun will always maintain the same height in the sky throughout the entire day, never rising or falling.

The calculation of the height of the sun, measured as $^\circ$ above the horizon (θ_h) is as follows:

$$\theta_h = \arcsin(\sin\theta_l \times \sin\theta_d + \cos\theta_l \times \cos\theta_d \times \cos\theta_t) \quad \text{Eqn. 1}$$

where, as mentioned above,

θ_l = observer's latitude

θ_d = sun's declination

θ_t = hour-angle of the sun

Light energy is absorbed and scattered by particles and molecules in the earth's atmosphere. Three variables are important in describing atmospheric transmission: the quality of the atmospheric composition, the path length travelled through the atmosphere and the wavelength of the light ray. The variables describing the quality of the atmosphere are too numerous to evaluate adequately, so empirical observations are utilized in the description of atmospheric attenuation.

Astronomers describe the intensity of a light source in units of magnitude, m . This is an exponential scale, in which a light source of magnitude 2 is actually 2.51 times brighter than a light source of magnitude 3, and is 2.51^2 times brighter than a source of

magnitude 4, etc. Blanco and McCusky (1961) show an equation for the change in magnitude, Δm , of a light source passing through the atmosphere:

$$\Delta m = 1.085T_0 \sec z$$

where $1.085T_0$ is empirically determined, ($1.085T_{0440nm} = 0.22$;

$1.085T_{0660nm} = 0.09$), and z equals the angle of incidence of light striking the earth's upper atmosphere ($90 - \theta_h$).

For 440nm light,

$$\Delta m = 0.22 \sec(90 - \theta_h)$$

and for 660nm light,

$$\Delta m = 0.09 \sec(90 - \theta_h)$$

We are principally interested in the percentage transmission of light at a given wavelength. This can be achieved knowing Δm , even without knowing m itself. Recalling exponential functions.

$$\frac{a^{x-y}}{a^x} = a^{x-y-x} = a^{-y}$$

for all a , x and y .

Substituting for a the base 2.51, and for y , the value of m , we find that

$$\text{transmission} = 2.51^{-(\Delta m)}$$

and further substituting for Δm ,

$$\text{transmission}_{440\text{nm}} = 2.51^{-(0.22\sec(90-\theta_h))} \quad \text{Eqn. 2}$$

and

$$\text{transmission}_{660\text{nm}} = 2.51^{(0.09\sec(90-\theta_h))} \quad \text{Eqn. 3}$$

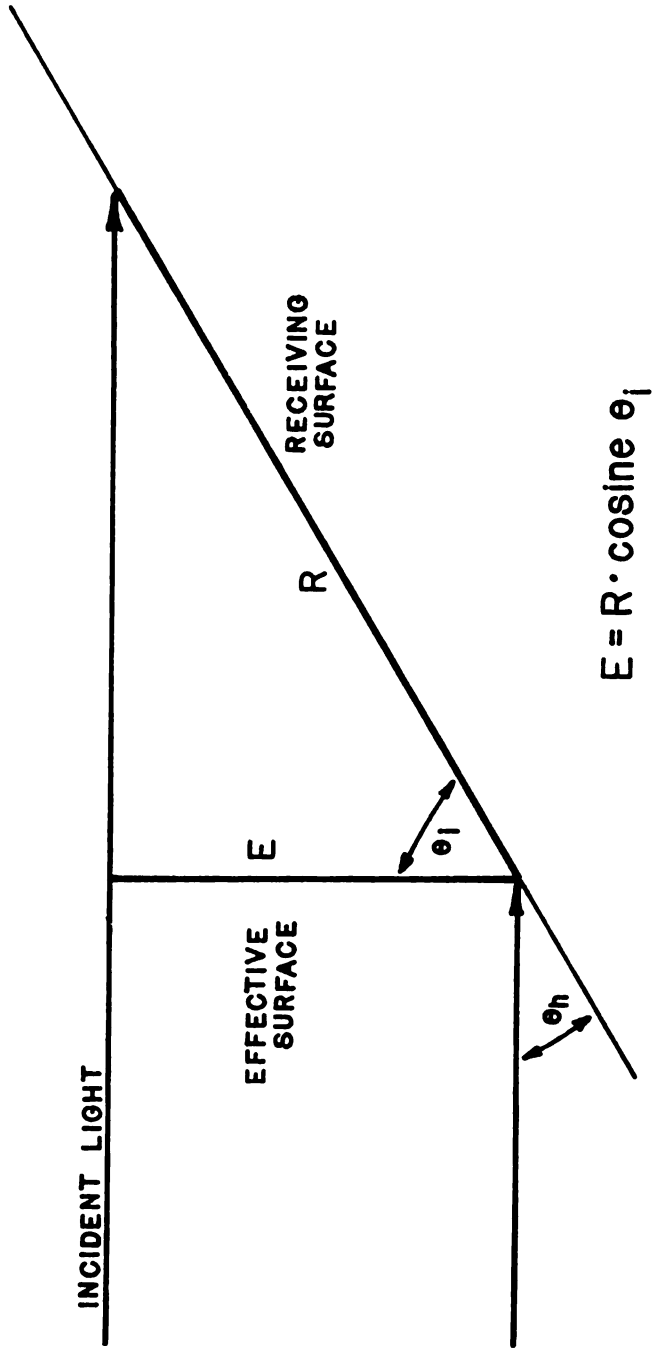
Measurement of the estimate of light energy transmitted through the earth's atmosphere has been expressed in relation to a surface perpendicular to the path of the light. One square centimeter of lake surface has an effective absorbing surface of one square centimeter only when the light path is perpendicular to the lake surface. At other times the effective surface of absorption will be smaller than the receiving surface. Figure A3 shows the relation between the angle of incidence of light and the effective absorbing area of a receiving surface. This relation provides:

$$\text{IRR}_w = \text{IRR}_n \times \cos\theta_i \quad \text{Eqn. 4}$$

where IRR_w = irradiance on the water surface ($\text{cal}/\text{cm}^2/\text{min}$)
 IRR_n = irradiance on a surface normal to the incoming light ($\text{cal}/\text{cm}^2/\text{min}$)
 θ_i = angle of incidence of the incoming light

Because the speed of light is slightly different in various media, the path of light rays are changed as they pass from one medium to another. This phenomenon is called refraction, and the relative speeds of light in various media determine the refractive indices. For air, the refractive index, N_{air} , is 1.00029. For

Figure 3.--The effective absorbing area of a receiving surface when the angle of incidence is non-zero.



water, the refractive index, N_{water} , is 1.33. Figure A4 shows the path of an incoming ray of light, which is described by its angle of incidence, θ_i . Note that $\theta_i = 90 - \theta_h$. The angle of refraction, called θ_r , determines the path of the light ray through the water.

Using Snell's law,

$$N_{\text{air}} \sin \theta_i = N_{\text{water}} \sin \theta_r$$

and since $N_{\text{air}} \sim 1$,

$$\sin \theta_i = N_{\text{water}} \sin \theta_r$$

and

$$\sin \theta_r = \frac{\sin \theta_i}{N_{\text{water}}}$$

giving

$$\theta_r = \arcsin\left(\frac{\sin \theta_i}{N_{\text{water}}}\right)$$

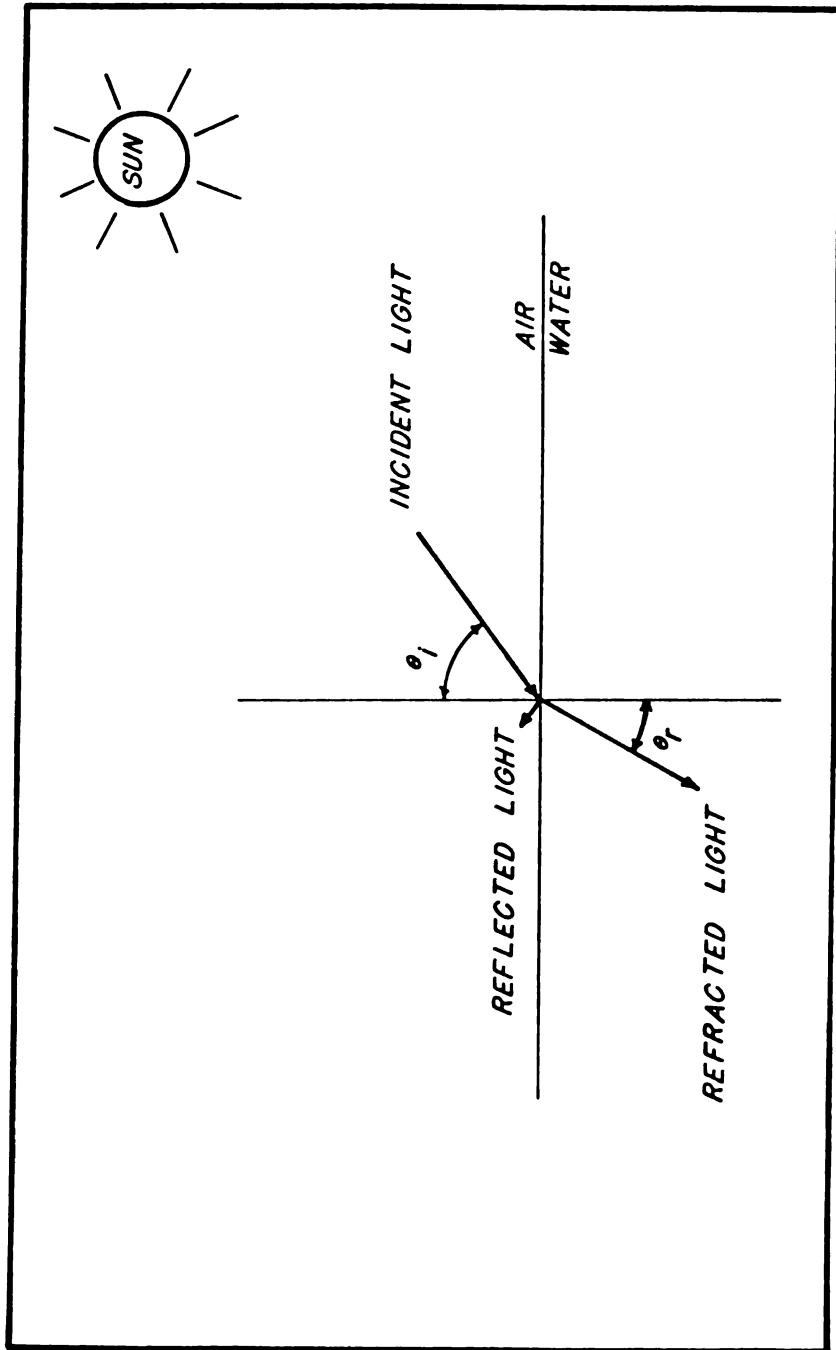
Substituting for N_{water} , we find that

$$\theta_r = \arcsin\left(\frac{\sin \theta_i}{1.33}\right) \quad \text{Eqn. 5}$$

As the angle of incidence of light rays increases, the reflection of light at the air-water interface increases. According to Fresnel's Law,

$$\text{Reflection} = R = \frac{1}{2} \left(\frac{\sin^2(\theta_i - \theta_r)}{\sin^2(\theta_i + \theta_r)} + \frac{\tan^2(\theta_i - \theta_r)}{\tan^2(\theta_i + \theta_r)} \right) \quad \text{Eqn. 6}$$

Figure A4.--Refraction of light at the air-water interface, showing the relationships of incident, reflected and refracted light.



Just as light passing through the atmosphere is diminished, so is light passing through water. The Beer-Lambert Law describes the extinction of light by water as follows:

$$I_z = I_0 e^{-nz} \quad \text{Eqn. 7}$$

where I_z is the intensity of the light ray after travelling z meters through the water, and I_0 is the initial intensity of light ray, which will herein be defined as 1.0; n is the extinction coefficient for water, for a specified wavelength.

In calculating the attenuation of light by water of a particular depth, it is necessary to determine the path length of light rays to the depth level, as dependent upon the angle of refraction of the light ray. The path length, z , of light to a given depth, d , is given by:

$$z = \frac{d}{\cos\theta_r} \quad \text{Eqn. 8}$$

where θ_r is the angle of refraction of light entering the water.

These equations can be successively iterated to approximate the theoretical maximum irradiance reaching a specified depth of water for lakes of any latitude. Integration can be performed over short time intervals to estimate peak rates of irradiance and over longer intervals to estimate daily total or seasonal total irradiance.

RESULTS

A sample calculation is shown below for light in the 440-450 nm waveband, travelling to the 2-meter depth at Harding Lake, Alaska (64° 25' N. Lat.) on June 8 at 1500 hours.

Irradiance in the 440-450 nm waveband is estimated by referring to Figure A1. To read this graph, the wavelengths must be converted to frequencies in cm^{-1} :

$$440 \text{ nm} = 4.4 \times 10^{-7} \text{ m}$$

and

$$450 \text{ nm} = 4.5 \times 10^{-7} \text{ m}$$

inverting each, we obtain:

$$(440) \quad 1/4.4 \times 10^{-7} = 2.273 \times 10^6 \text{ m}^{-1}$$

$$(450) \quad 1/4.5 \times 10^{-7} = 2.222 \times 10^6 \text{ m}^{-1}$$

converting to cm^{-1} :

$$(440) \quad 2.273 \times 10^6 \text{ m}^{-1} \times 10^{-2} \frac{\text{cm}^{-1}}{\text{m}^{-1}} = 22,730 \text{ cm}^{-1}$$

$$(450) \quad 2.222 \times 10^6 \text{ m}^{-1} \times 10^{-2} \frac{\text{cm}^{-1}}{\text{m}^{-1}} = 22,222 \text{ cm}^{-1}$$

So, the bandwidth (440-450) is

$$22,730 - 22,222 = 508 \text{ cm}^{-1}$$

From the graph we see that in this band the irradiance is about $7 \times 10^{-5} \text{ cal/cm}^2/\text{min/cm}^{-1}$. Multiplying by bandwidth,

$$508 \text{ cm}^{-1} \times 7 \times 10^{-5} \text{ cal/cm}^2/\text{min/cm}^{-1} = 0.0356 \text{ cal/cm}^2/\text{min}$$

which strikes the earth's upper atmosphere in the 440-450 nm waveband.

To estimate attenuation of this incident solar irradiance along its path to the aquatic system, the sun's elevation in the sky is calculated:

First, θ_1 is given as $64^\circ 25'$ N. Lat. Converted to a decimal fraction,

$$\theta_1 = 64.41^\circ$$

Looking in Table A1, on June 8,

$$\theta_d = 22.84^\circ$$

And finally, at 1500 hours,

$$\theta_t = 45^\circ$$

Then, solving Eqn. 1,

$$\theta_h = \arcsin(\sin 64.41^\circ \sin 22.84^\circ + \cos 64.41^\circ \cos 22.84^\circ \cos 45^\circ)$$

$$= \arcsin(0.90 \times 0.39 + 0.43 \times 0.92 \times 0.71)$$

$$= \arcsin(0.63)$$

$$\theta_h = 39.19^\circ$$

The path of the sun through the sky varies considerably on any day among the latitudes. Figure A5 illustrates the path of the sun for the solstice day at Harding Lake and at Lake Lansing, Michigan (42° 25' N. Lat.).

Solving for atmospheric transmission at Harding Lake, June 8, 1500 hours:

$$\theta_h = 19.19^\circ$$

so, by Eqn 2:

$$\begin{aligned} T_{440\text{nm}} &= 2.51^{-(0.22\text{sec}(90 - 39.19))} \\ &= 2.51^{-(0.22 \times 1.58)} \\ &= 2.51^{-.35} \\ &= 0.72 \end{aligned}$$

Similarly, by Eqn. 3,

$$\begin{aligned} T_{660\text{nm}} &= 2.51^{-(0.09\text{sec}(90 - 39.19))} \\ &= 0.88 \end{aligned}$$

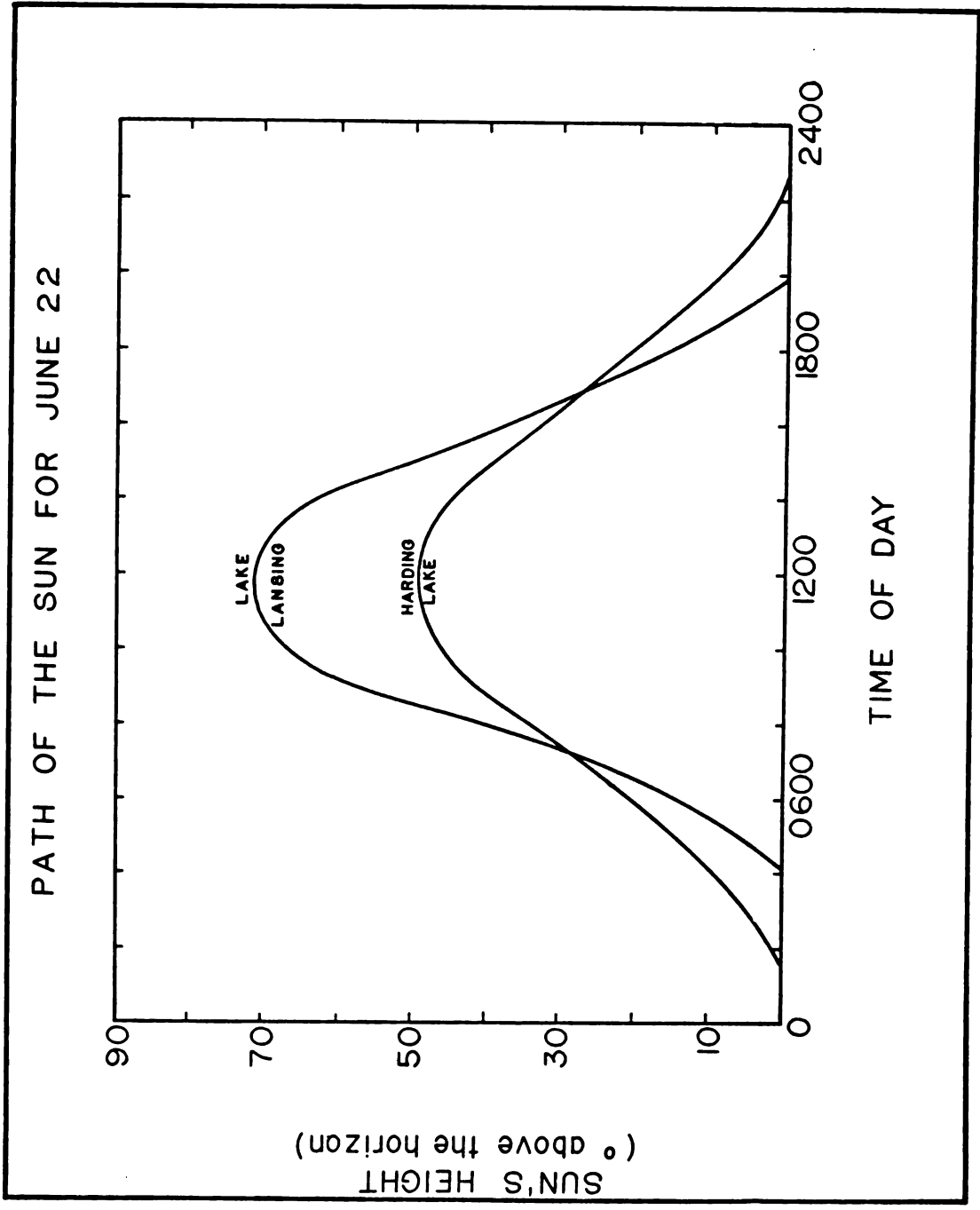
Using the atmospheric transmission value for 440 nm light, we estimate that in the 440-450 nm waveband,

$$0.72 \times 0.0356 \text{ cal/cm}^2/\text{min}$$

or

$$0.0266 \text{ cal/cm}^2/\text{min}$$

Figure A5.--Path of the sun through the sky on June 22 at
Harding Lake and Lake Lansing.



reaches the lake's surface if the angle of incidence were 0.
Correcting for the non-zero angle of incidence, by Eqn. 4:

$$\begin{aligned} \text{IRR}_i &= 0.0256 \text{ cal/cm}^2/\text{min} \times \cos(50.81) \\ &= 0.0162 \text{ cal/cm}^2/\text{min} \end{aligned}$$

where IRR_i is the irradiance striking the Harding Lake surface.

To estimate the reflection at the lake's surface, we first calculate the angle of refraction, using Eqn. 5:

$$\theta_r = \arcsin\left(\frac{\sin(90-\theta_h)}{1.33}\right)$$

and since $\theta_h = 39.19$,

$$\begin{aligned} \theta_r &= \arcsin\left(\frac{\sin(50.81)}{1.33}\right) \\ &= \arcsin(0.58) \end{aligned}$$

thus,

$$\theta_r = 35.64^\circ$$

We then calculate reflection, R, by Eqn. 6:

$$\theta_r = 35.64^\circ$$

then

$$(\theta_i - \theta_r) = 15.17^\circ$$

and

$$(\theta_i + \theta_r) = 86.45^\circ$$

therefore,

$$\begin{aligned}
 R &= \frac{1}{2} \left(\frac{\sin^2(15.17)}{\sin^2(86.45)} + \frac{\tan^2(15.17)}{\tan^2(86.45)} \right) \\
 &= \frac{1}{2} \left(\frac{0.07}{1.00} + \frac{0.07}{259.8} \right) \\
 &= \frac{1}{2}(0.07)
 \end{aligned}$$

and

$$R = 0.035$$

The irradiance entering the water is estimated as follows:

$$\text{IRR}_e = \text{IRR}_i \times (1 - R)$$

where

IRR_e = irradiance entering the water

IRR_i = irradiance incident to the water

R = reflection

Then,

$$\begin{aligned}
 \text{IRR}_e &= 0.0162 \times (1 - 0.035) \text{ cal/cm}^2/\text{min} \\
 &= 0.0156 \text{ cal/cm}^2/\text{min}
 \end{aligned}$$

entering Harding Lake.

Before calculating the attenuation of light by the water, it is necessary to determine the length of the path the light will travel to reach the 2-meter depth. By Eqn. 8:

$$\begin{aligned}
 z &= \frac{2}{\cos\theta_r} \text{ meters} \\
 &= \frac{2}{\cos(35.64)} \text{ meters} \\
 &= 2.46 \text{ meters}
 \end{aligned}$$

To calculate the extinction of 440-450 nm light by the water, we use an extinction coefficient, n , of 0.272. So, by Eqn. 7:

$$\begin{aligned}
 I_{2.46} &= e^{-nz} \\
 &= e^{-0.0078 \times 2.46} \\
 &= e^{-0.02} \\
 &= 0.98
 \end{aligned}$$

Then to estimate irradiance at the 2-meter depth in Harding Lake, June 8, 1500 hours,

$$\begin{aligned}
 \text{IRR}_{2m} &= \text{IRR}_e \times 0.98 \\
 &= 0.0156 \times 0.98 \text{ cal/cm}^2/\text{min} \\
 &= 0.0153 \text{ cal/cm}^2/\text{min}
 \end{aligned}$$

The above calculations have been performed for each 10 degrees of latitude from the equator to the north pole. The equations were iterated every 6 minutes through the entire 24-hour period of the summer solstice day. The irradiance in the 440-450 and

660-670 nm wavebands at the 0-meter and 4-meter depths were determined, using extinction coefficients for Crystal Lake, Wisconsin (calculated from Wetzel, 1975). The true color of the lake is 0 pt units (Wetzel, 1975). The computer program which generated these values is shown in Appendix II.

The path of the sun through the sky varies considerably with latitude. Figure A6 shows the sun's elevation during the summer solstice day throughout the northern hemisphere. Figure A7 describes the irradiance in each waveband for each depth as it varies with the sun's elevation in the sky. Figure A8 provides an integration of all variables to determine the total daily irradiance in each waveband at each depth as it varies with latitude.

While daylength increases with latitude during the summer months, the maximum rates of irradiance decrease for any depth. The highest total irradiance to the 0-meter depth is found in the mid-temperate latitudes on the solstice day. The similar total for the 4-meter depth is found in the sub-tropical latitudes.

Figure A6.--Path of the sun through the sky on the summer solstice
day throughout the northern hemisphere.

THE SUN'S PATH
ON THE
SUMMER SOLSTICE

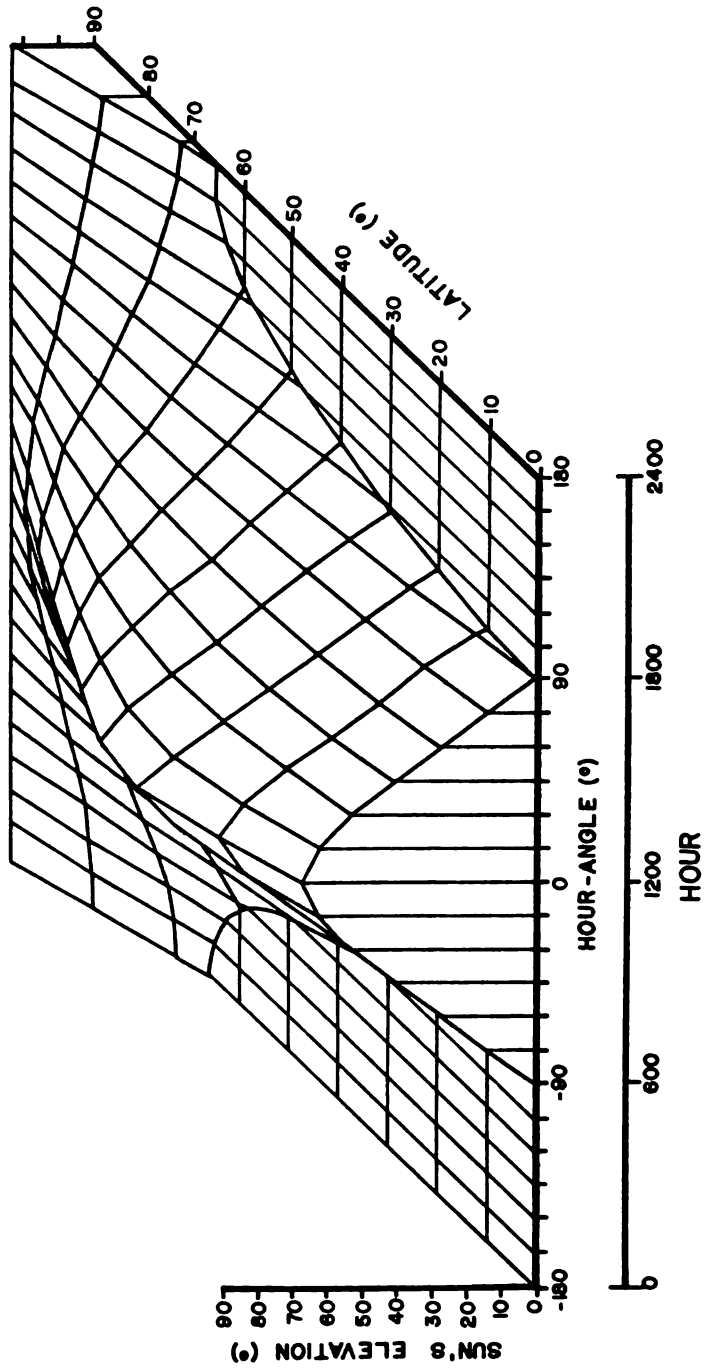


Figure A7.--The influence of the sun's angular elevation on the solar irradiance at 440-450 and 660-670 nm which reaches the 0- and 4-meter depths in lakes. ($n_{440} = 0.272$; $n_{660} = 0.516$)

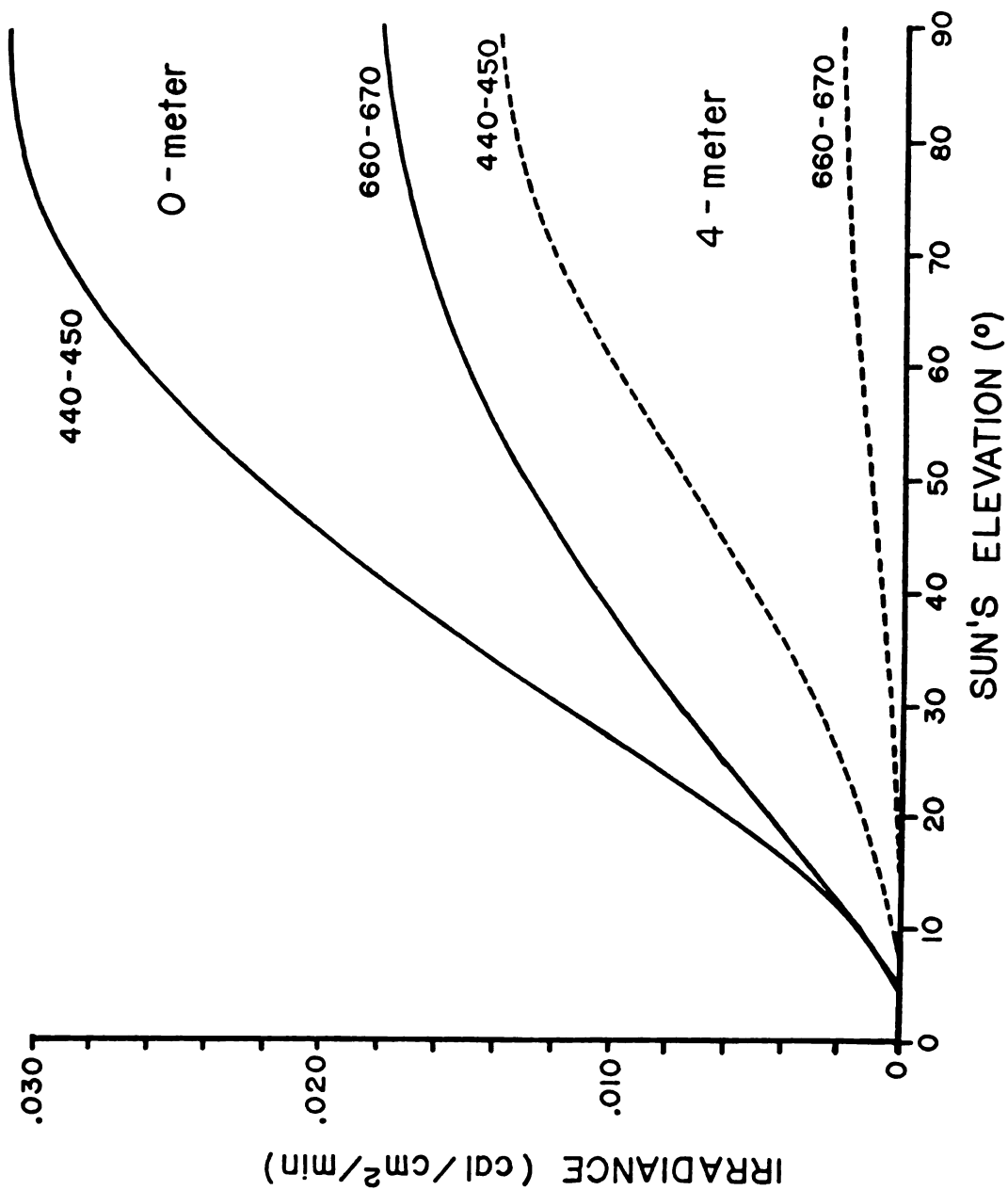
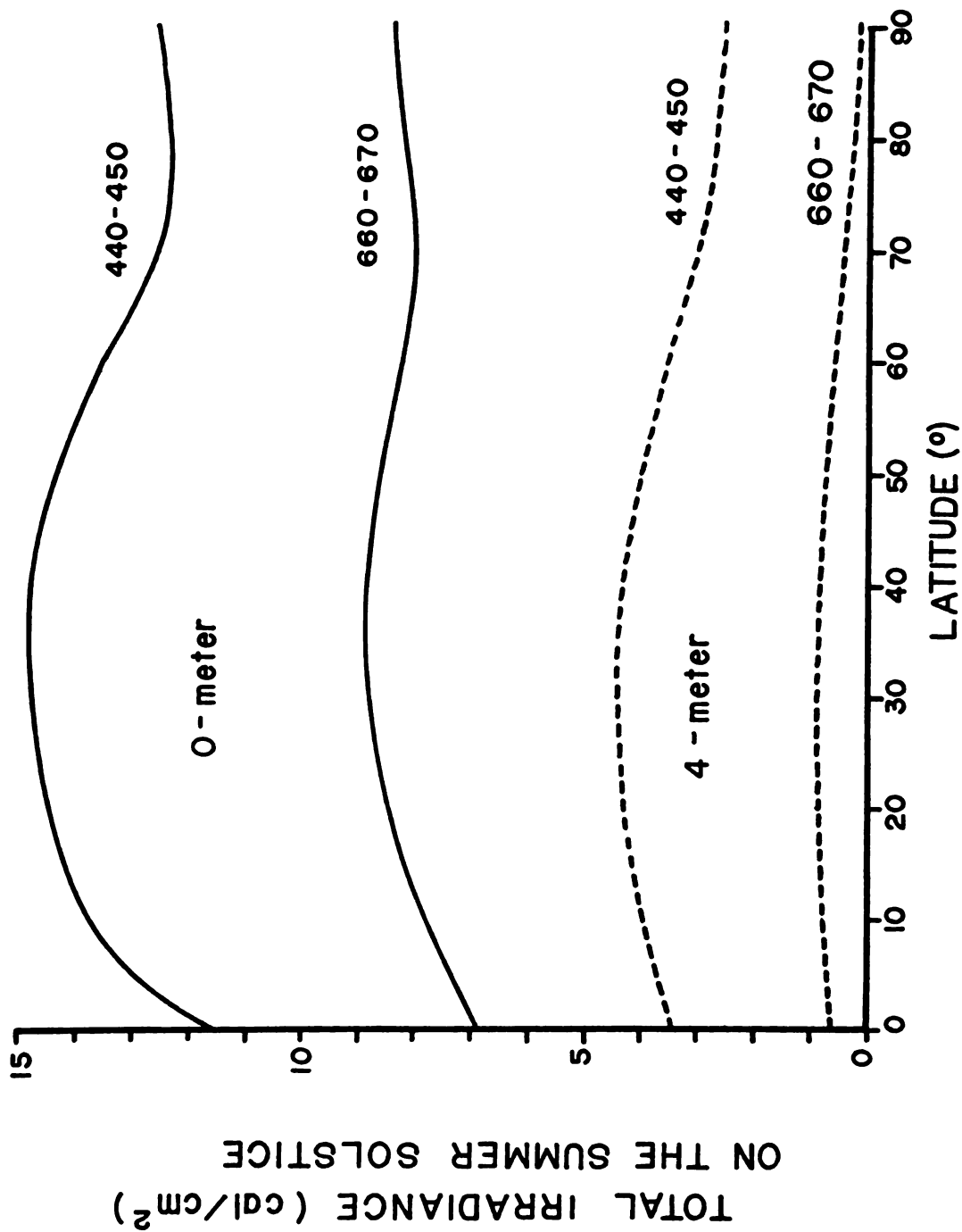


Figure A8.--Total solar irradiance in the 440-450 and 660-670 nm wavebands which reaches the 0- and 4-meter depths of lakes at all latitudes of the northern hemisphere on June 22 ($n_{440} = 0.272$; $n_{660} = 0.516$).



DISCUSSION

Solar irradiance has long been considered a principle variable in the description of aquatic habits. Although the model presented here describes only the maximum potential solar irradiance, the importance of these calculations in aquatic ecology may be great. Hutchinson (1975) cites data from Finnish lakes which shows the relation of the maximum depth of macrophyte growth to Secchi disk transparency of the water. The model presented here leads to the expectation that if the Finnish studies were expanded over a wide latitude gradient, the relation cited by Hutchinson (1975) would become much less obvious. It should be possible, though, to calculate the daily total irradiance at the maximum macrophyte depth to discover the relation between this depth and actual solar irradiance levels.

Spence and Chrystal (1970a,b) determined that the depth zonation of vascular hydrophyte species populations was directly related to solar irradiance levels and the light or shade tolerances of the species. The model presented here leads to the expectation that the depth zonation patterns established by Spence and Chrystal (1970a,b) would be found at increasingly shallower depths with increasing latitude above the tropics.

The close examination of existing hypotheses on the interrelation of light and plant growth as presented by Hutchinson,

Spence and Chrystal, and others, with the aid of the solar irradiance prediction calculations shown in this paper may cause their modification or elimination, or add strength to them by removing the latitude as a source of variability.

LITERATURE CITED

LITERATURE CITED

- Blanco, V. M., and S. W. McCusky. 1961. Basic Physics of the Solar System. Addison-Wesley, Reading, Massachusetts. 307+xi pp.
- Gates, D. M. 1962. Energy Exchange in the Biosphere. Harper and Row, New York. 151 pp.
- Hutchinson, G. E. 1975. A Treatise on Limnology, Vol. III. Limnological Botany. Wiley Interscience, New York. 660+x pp.
- Spence, D. H. N. and J. Chrystal. 1970a. Photosynthesis and zonation of freshwater macrophytes. I. Depth distribution and shade tolerance. *New Phytol.* 69:205-215.
- _____. 1970b. Photosynthesis and zonation of freshwater macrophytes. II. Adaptability of species of deep and shallow water. *New Phytol.* 69:217-227.

APPENDIX II

COMPUTER PROGRAM FOR THE CALCULATION
OF POTENTIAL ENERGY INPUTS TO LAKES

FORTRAN STATEMENT

LINE

```

1      PROGRAM LITE(INPUT,OUTPUT,TAPE1=INPUT,TAPE2=OUTPUT)
C     TYPE STATEMENTS
      REAL LAT
      INTEGER PCHECK
5     C SET DEBUGGING SWITCH
      NBUG=0
C     READ VALUES FOR DAY NUMBER, DECLINATION, AND EXTINCTION COEFFICIENTS
      READ(1,5) NDAY,DEC,EX440,EX660
      5 FORMAT(1X,I3,/,4(1X,F10.5,/))
10    C GENERATE DEPTH VALUES OF 0, 2, AND 4 METERS
      DO 50 J=1,3
C     CHECK DEBUGGING SWITCH
      IF(J.GT.1.AND.NBUG.EQ.1) GO TO 50
C     SET DEPTH VALUES
      IF(J.EQ.1) DEPTH =0.
      IF(J.EQ.2) DEPTH =2.
      IF(J.EQ.3) DEPTH =4.
C     GENERATE LATITUDES VALUES FROM 0 TO 80 DEGREES BY 10-DEGREE INCREMENTS
      DO 40 N=1,9
20    LAT=10.0*(N-1)
C     INITIALIZE CONSTANTS
C     SOL440 -- THE RATE OF SOLAR ENERGY INPUT TO THE EARTHS UPPER STMOSPHERE
      IN THE 440 TO 450 NM WAVEBAND DURING A SIX-MINUTE PERIOD
      SOL440=.2376
25    C     SOL660 -- THE RATE OF SOLAR ENERGY INPUT TO THE EARTHS UPPER ATMOSPHERE
      IN THE 660 TO 670 NM WAVEBAND DURING A SIX-MINUTE PERIOD
      SOL660=.1188
C     PI
      PI=3.141592654

```

FORTRAN STATEMENTLINE

```

30 C PI/2
    PI2=PI/2
C E -- THE NATURAL LOG BASE
    E=2.718281828
35 C DTOR -- THE CONVERSION FACTOR FROM DEGREES TO RADIAN MEASURE
    DTOR=.017453293
C RTOD -- THE CONVERSION FACTOR FROM RADIAN MEASURE TO DEGREES
    RTOD= 57.29577951
C INITIALIZE ENERGY ACCUMULATION VARIABLES
    ETOT440=0
    ETOT660=0
40 C TRANSLATE INPUT VARIABLES TO RADIAN MEASURE
    RDEC=DEC*DTOR
    RLAT=LAT*DTOR
45 C SET COLUMN HEADING PRINT CHECKER
    PCHECK=75
C GENERATE HOUR-ANGLE VALUES
    DO 10 I=1,241
    HANGL=-181.5+I*1.5
    RHANGL=HANGL*DTOR
50 C CALCULATE ANGULAR HEIGHT VALUES
    A=SIN(RDEC)*SIN(RLAT)
    B=COS(RDEC)*COS(RLAT)*COS(RHANGL)
    RANGLHT=ASIN(A+B)
C CALCULATE RADIAN ANGLE OF INDINCENCE
    RINC=P12-RANGLHT
55 C CONVERT TO DEGREE MEASURE
    AINC=RINC*RTOD
    ANGLHT=RANGLHT*RTOD
C AVOID FURTHER CALCULATIONS WHEN ANGLHT IS LESS THAN 3 DEGREES
    IF(ANGLHT.LT.3) GO TO 10
60

```

LINEFORTRAN STATEMENT

```
65 C CALCULATE ATMOSPHERIC TRANSMISSION AT EACH WAVELENGTH
    AT440=2.51**(-.22*(1/COS(RINC)))
    AT660=2.51**(-.09*(1/COS(RINC)))
C CALCULATE ENERGY TRANSMISSION TO THE WATER SURFACE
  T440=SOL440*AT440
  T660=SOL660*AT660
C CORRECT FOR NON-ZERO AINC
  T440=T440*COS(RINC)
  T660=T660*COS(RINC)
70 C CALCULATE ANGLE OF REFRACTION
    REFRAC=ASIN(SIN(RINC)/1.33)
C CALCULATE REFLECTION
  D=RINC-REFRAC
  S=RINC+REFRAC
75 REFLEC=.5*(SIN(D)**2/SIN(S)**2+(SIN(D)/COS(D))**2/(SIN(S)/COS(S))*
  +*2)
C ESTIMATE LIGHT ENERGY ENTERING WATER
  T440=T440*(1-REFLEC)
  T660=T660*(1-REFLEC)
80 C ESTIMATE PATH LENGTH OF THE LIGHT THROUGH THE WATER
    Z=DEPTH/COS(REFRAC)
C CALCULATE TRANSMISSION BY WATER
  WAT440=E**(-1.*Z*EX440)
  WAT660=E**(-1.*Z*EX660)
  T440=T440*WAT440
  T660=T660*WAT660
85 C ACCUMULATE DAILY TOTAL IRRADIANCES
    ETOT440=ETOT440+T440
    ETOT660=ETOT660+T660
```

LINEFORTRAN STATEMENT

```
90 C CHECK FOR HEADING PRINT -- IF NOT, GO TO DATA PRINT
    IF(PCHECK.NE.75) GO TO 20
95 C RESET PCHECK BEFORE PRINTING COLUMN HEADINGS
    PCHECK=0
    C PRINT COLUMN HEADINGS
      WRITE(2,16) NDAY,DEC,RDEC,LAT,RLAT,EX550,EX660,DEPTH
      16 FORMAT(1H1,*NDAY*,3X,*DEC*,6X,*REC*,7X,*LAT*,6X,*RLAT*,6X,*EX440*
        +,5X,*EX660*,5X,*DEPTH*/,1X,I3,7F10.5)
        WRITE(2,17)
      17 FORMAT(1H0,*INT HANGL ANGLHT AINC AT440 AT660 REFRAC REFLEC Z W
        +AT440 WAT660 T440 ETOT 440 T660 ETOT660*)
    C PRINT DATA
      20 WRITE(2,21) I,HANGL,ANGLHT,AINC,AT440,AT660,REFRAC,REFLEC,Z,WAT440
        +,WAT660,T440,ETOT440,T660,ETOT660
      21 FORMAT(1X,I3,1X,F6.1,2(1X,F5.2),4(1X,F5.4),1X,F5.w,2(1X,F5.4),4(1X
        +,F7.4))
    C END LIGHT ENERGY CALCULATION LOOP
    10 CONTINUE
    C END LATITUDE GENERATION LOOP
    40 CONTINUE
    C END DEPTH GENERATION LOOP
    50 CONTINUE
    C END PROGRAM
      END
```

MICHIGAN STATE UNIV. LIBRARIES



31293106691524